THE UNIVERSITY OF OKLAHOMA

GRADUATE COLLEGE

THERMOLUMINESCENT RESPONSE OF LITHIUM FLUORIDE TO HIGH ENERGY PHOTONS

A DISSERTATION

SUBMITTED TO THE GRADUATE FACULTY

in partial fulfillment of the requirements for the degree of

DOCTOR OF PHILOSOPHY

BY

ALEXANDER PENDLETON TURNER

Norman, Oklahoma

1971

THERMOLUMINESCENT RESPONSE OF LITHIUM FLUORIDE TO HIGH ENERGY PHOTONS

APPROVED BY

Robert J. Nelson

David N. Anderson

Larry Carter

James M. Coleman

DISSERTATION COMMITTEE

ACKNOWLEDGEMENTS

The author would like to express his appreciation to Dr. Robert Y. Nelson for his guidance and encouragement. The suggestions by Dr. Larry W. Canter and Dr. James M. Robertson were most helpful. A special thanks is given to Dr. David W. Anderson for his continuing advice and assistance during the performance of this study.

The author is indebted to his wife, Karen, for her continuing encouragement, understanding, and assistance. A final note of appreciation is due Mr. Charles E. Smith of M.D. Anderson Hospital and Tumor Institute for his advice and assistance, and for making available the use of the hospital facilities.

This work was done in partial fulfillment of the requirements for the degree of Doctor of Philosophy from the University of Oklahoma.

TABLE OF CONTENTS

LIST OF TABLES

LIST OF ILLUSTRATIONS

THERMOLUMINESCENT RESPONSE OF LITHIUM FLUORIDE TO HIGH ENERGY PHOTONS

CHAPTER I

INTRODUCTION

The unique properties of lithium fluoride have made it the most widely used thermoluminescent dosimeter material. Some of the properties that have made this material suitable for all areas of radiation dosimetry have been well documented and include wide range of exposures, dose rate independence, approximate tissue equivalence, long term response retention, accurate measurement of various quality radiations, approximation of an ideal "point detector," high precision, and essential energy independence. These properties make lithium fluoride extremely useful in medicine and the sciences where the quantity of absorbed dose in a medium is desired.

Ideally, a dosimetry system for measuring absorbed dose in a medium should have a flat response with energy, because the energy of exposure can vary over a wide range and the energy spectrum within a medium will vary for a given exposure. Although lithium fluoride has a relatively flat energy response when compared to other dosimetry systems, it does exhibit a noticeable energy dependence at low kilovoltage energies. Published reports on thermoluminescent response of

lithium fluoride to energies in this range are consistent and all verify this dependence.

With the increasing use of megavoltage radiation in medicine, it is important that the thermoluminescent response of lithium fluoride be well understood in this higher range. At megavoltage energies, the response of lithium fluoride has been generally assumed to be flat. However, several recent investigations have been oriented to the thermoluminescent response of lithium fluoride to X-ray and electron energies to 35 Mev. Reports of these works are not consistent. Several investigators have reported a decrease in response with increasing energy, whereas others have not observed this decrease.

The purpose of this study was therefore to investigate the thermoluminescent response of lithium fluoride to megavoltage photon radiation and to extend the current information to 65 Mev.

A thermoluminescent dosimeter made of 100% lithium fluoride with dimensions of 1 mm x 1 mm x 6 mm is widely used in radiation therapy dosimetry. For this reason, this form of lithium fluoride was selected for this study.

The radiation source was a 70 Mev synchrotron operated by the Department of Radiological Sciences of the University of Oklahoma Medical Center. The X-ray beam from this machine was used to irradiate a semi-infinite water phantom in which the dosimeters were placed.

Thermoluminescent and ferrous sulfate dosimeters were irradiated simultaneously at the following energies: 35 Mev, 50 Mev, and 65 Mev. They were positioned in the phantom at the depth of maximum dose for each energy. The ferrous sulfate dosimeters were used to establish the thermoluminescent response per rad of absorbed dose at each energy. These values were then normalized by the thermoluminescent response per rad of absorbed dose to cobalt-60 gamma irradiation to establish the effect of increasing photon energy on thermoluminescent response.

CHAPTER II

THERMOLUMINESCENCE

2.1 Physical Process

Although the fundamental theory of thermoluminescence is not fully known, the physical process is qualitatively understood. This has been documented by Schulman (1966), Fowler and Attix (1966), and Cameron *et al.* (1968). For the purpose of this study, however, a brief description of the physical process will be given as a refresher in the thermoluminescent process.

The energy lost when ionizing radiation is absorbed in matter predominately results in the excitation and ionization of orbital electrons. In lithium fluoride, the ionized electrons and the associated free holes can be trapped in metastable energy states before they have a chance to return to ground state and recombine. These trapping sites are localized defects and impurities within the lithium fluoride crystal lattice, and are attracted by coulombic forces to these charged particles.

Energy level models for thermoluminescence in lithium fluoride have been proposed by Cristy *et al.* (1967), and Mayhugh (1970). Although the overall models differ, the mechanisms proposed share one feature: that is, thermoluminescence occurs after electrons trapped at anion vacancies recombine with holes. These models show an energy barrier

of between 12 ev and 14 ev between the valence band and conduction band, and the energy level of trapped electrons is on the order of 6 ev below the conduction band. The thermoluminescent process is initiated when thermal energy is put into the lithium fluoride crystal. Ultimately, thermoluminescent photons are given off after the trapped electrons tunnel through the energy barrier to recombine with holes and return to ground state. Thus, the phenomenon of thermoluminescence stems from thermally stimulated release of light photons.

The probability of this mechanism is dependent on temperature; increasing with increasing temperature. The thermal energy required to initiate this process is large enough to prevent these trapped particles from returning to ground state at room temperature. By increasing temperature, a level will be reached where essentially all trapped electrons will be released to return to ground state. Therefore, increasing temperature will increase thermoluminescent output. It will pass through a maximum and then decrease with increasing temperature.

The temperature at which a given trap will empty is determined by the energy of the metastable state. Lithium fluoride has five such characteristic metastable states which require different levels of thermal energy for the release of trapped electrons and holes.

A plot of the light output, or thermoluminescence, as a

function of temperature is called a glow curve. A typical glow curve for lithium fluoride is shown in Figure 1. The different peaks in the glow curve indicate traps at different metastable energy levels peculiar only to lithium fluoride.

Zimmerman et al. (1966) found that after irradiation the peaks decay exponentially at room temperature with the following half-lives: peak 1-five minutes, peak 2-ten hours, peak 3-one-half year, peak 4-seven years, and peak 5-eighty years. Peaks 1 and 2 are not suitable for practical dosimetry since their half-lives would interfere with an attempted readout after irradiation. Peaks 3, 4, and 5 are therefore the most suitable for dosimetry due to their long half-lives.

The amplitude of the peaks indicates the relative proportion of trapped particles at that energy level. The shape of the glow curve is dependent on the heating rate and its uniformity; the size, shape, and thermal conductivity of the phosphor; the recording instrument used; the level of exposure; the type of radiation; the radiation and annealing history of the phosphor; and spurious effects. A complete survey of these effects has been documented by Cameron et al. (1968).

The usefulness of lithium fluoride as a radiation dosimeter is based on the fact that the light emitted when the phosphor is heated is a function of the number of trapped electrons and holes which, in turn, is determined by the radiation dose. The total thermoluminescence emitted is essentially constant per unit of radiation dose. The integrated

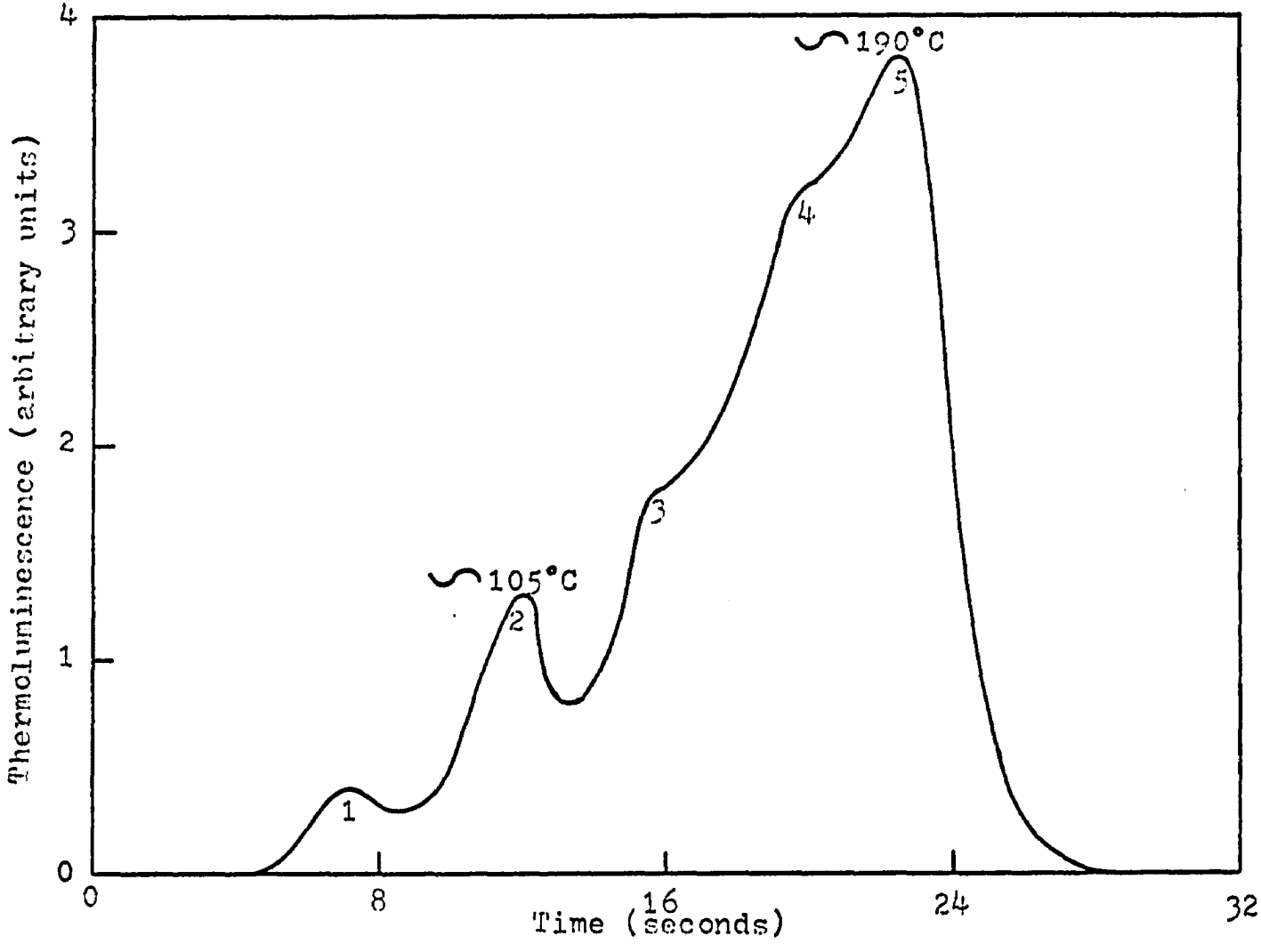

Figure 1. Typical Glow Curve of Lithium Fluoride TLD-100. The phosphor has been annealed 1 hour at 400°C and read soon after irradiation to 100 roentgens. (Zimmerman et al., 1966)

area under the glow curve is, therefore, a good reproducible measure of dose information.

2.2 Instrumentation

The instrumentation used in this study to determine the radiation dose received by lithium fluoride dosimeters was the Model TLR-5 Thermoluminescent Dosimeter Reader manufactured by Eberline Instrument Company. This is essentially a light measuring device which can supply controlled heat to the lithium fluoride dosimeters and record the integrated light output (Eberline Instrument Company, 1969).

The dosimeters are placed directly in a heater pan. When the readout cycle is initiated, the heater pan is brought up quickly to the preheat temperature and remains there for the duration of the preheat time. This automatically anneals out any unstable low temperature peaks incurred since the previous anneal. During this preheat time no light output is recorded.

At the end of the preheat time, the heater pan temperature is quickly increased to the readout temperature, which is constant during readout. A graphical representation of the entire readout cycle is shown in Figure 2. The light given off by the dosimeters during this time is sensed by the photomultiplier tube and converted to current. This current is then converted to pulses which are integrated over the readout time and registered on the display. The integrated pulse is proportional to the rate of light emission.

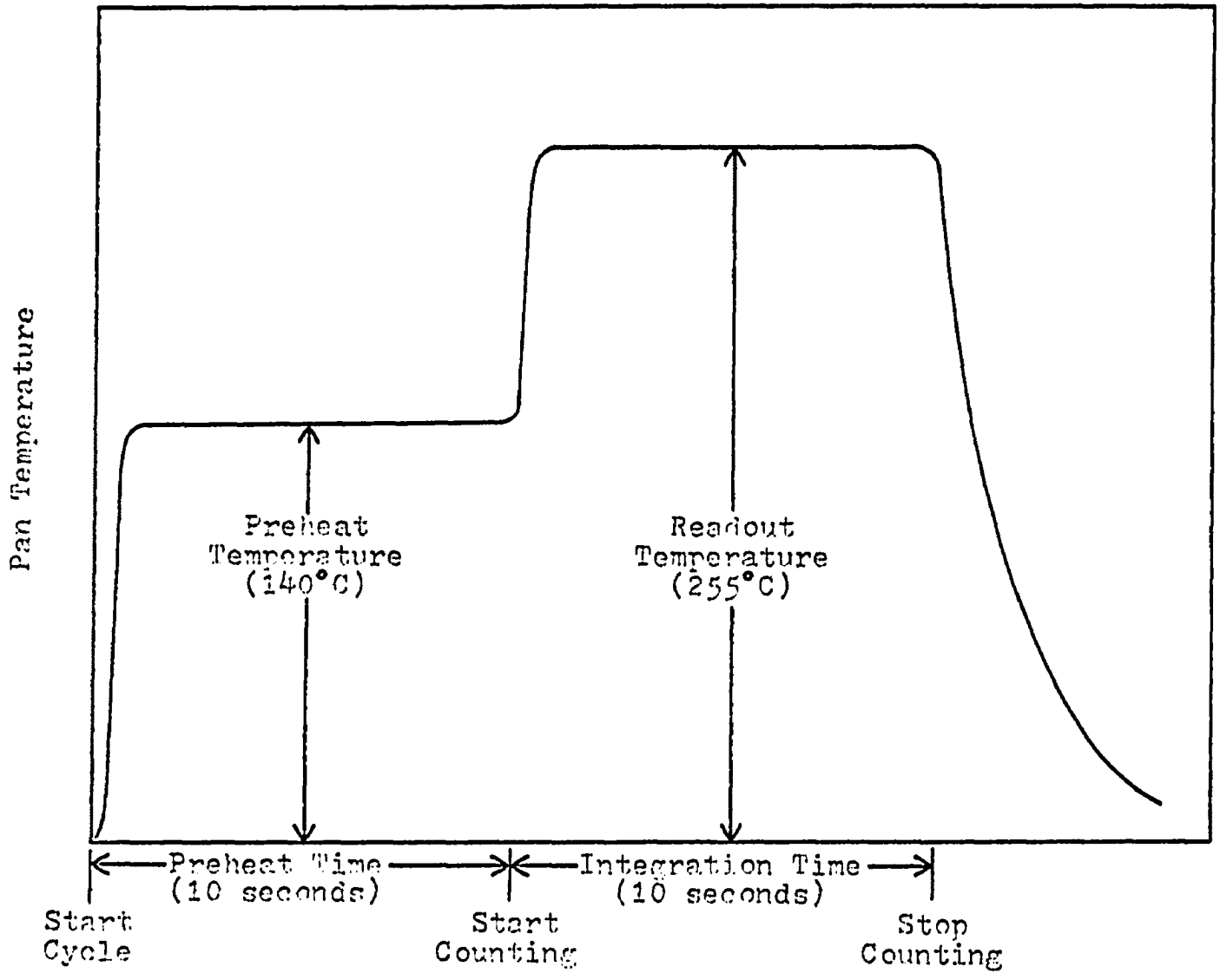

Figure 2. Lithium Fluoride Readout Cycle of Model TLR-5 Thermoluminescent Dosimeter Reader. (Eberline Instrument Company, 1969)

This instrument has a range from 1 mR to 10^5 R. The manufacturer lists instrument background at 25°C to be typically less than the equivalent of 10 mR.

The preheat and readout times and temperatures will depend on the type of thermoluminescent material used. For lithium fluoride, the manufacturer recommends the following range of settings:

Preheat time.....10 seconds
Preheat temperature.....140°C
Integration time.....10 seconds
Integration temperature.....255°C

The manufacturer also recommends for dose measurements of less than 10 R, 0.5 liters per minute of nitrogen gas should flow through the heater pan. This is necessary to reduce the non-radiation induced background thermoluminescence. Aitken et al. (1967) suggested that the removal of this background is due to the absence of oxygen rather than any specific quenching action of nitrogen. It was further proposed by Svarcer and Fowler (1967) that an oxygen atmosphere can modify the traps near the phosphor surface by the absorption of oxygen on the phosphor. Oxygen has a strong attraction for electrons and would therefore trap them by a strong energy bond. They found this idea consistent with the fact that the luminescence emitted from these oxygen saturated surfaces read out at a higher temperature than the radiation induced thermoluminescence.

With an oxygen atmosphere, the background for undosed lithium fluoride will typically give readings equivalent to

100-300 mR (Isotopes/Con-Rad, 1968). This can, however, be reduced to 5-25 mR with nitrogen gas. The standard deviation of these measurements decreased by an order of magnitude using nitrogen gas.

CHAPTER III

CHARACTERISTICS OF LITHIUM FLUORIDE

3.1 Dosimeters Used in Study

The lithium fluoride dosimeters used in this study were the 1 mm x 1 mm x 6 mm high sensitivity rods manufactured by Harshaw Chemical Company. These dosimeters are made with 100% lithium fluoride under conditions of controlled temperature and pressure. In addition to the characteristics listed later in this chapter, they are optically transparent, rugged, and easy to handle. Their size, composition, and characteristics made them ideal for this study.

Two types of rods, based on the isotopic abundance of lithium fluoride, were used. Harshaw quotes the compositions as follows: TLD-100 contains 7.5% lithium-6 and 92.5% lithium-7, and TLD-700 contains 0.007% lithium-6 and 99.993% lithium-7. The use of these two types of lithium fluoride enabled the discrimination of neutron and photon exposures. This technique is discussed later in this chapter.

3.2 Point Detector

Only a few milligrams of lithium fluoride are required in order to make a measurement (Endres, 1965). The Harshaw high sensitivity rods (1 mm x 1 mm x 6 mm) contain approximately 16 mg of lithium fluoride. This volume is several orders of magnitude less than other types of dosimeters and can be considered a "point detector" for many applications.

3.3 High Sensitivity

Harshaw quotes the measured standard deviation in thermoluminescent sensitivity within a given batch of high sensitivity rods to be between 2% and 4% of the mean at 1 roentgen exposure. A greater sensitivity than these values can be obtained by matching dosimeters of like mean response within the batch used.

3.4 Tissue Equivalent

The effective atomic number for photoelectric absorption in lithium fluoride is 8.14. This compares favorably with air (Z = 7.64), and tissue and water (Z = 7.42). The ratios between the mass absorption coefficients for lithium fluoride, air, tissue, and water vary relatively little with photon energy, so the response of lithium fluoride can be considered a close approximation of the dose received by an equal volume of the other materials when exposed under like conditions. At low energies, however, an exaggerated response should be expected due to an increase in the photoelectric cross section. When a high degree of accuracy is desired, corrections should be made for photon energy dependence.

3.5 Exposure Retention

The rate at which thermoluminescence is released from lithium fluoride is dependent on temperature. This rate increases with increasing temperature. There is, however, a measurable loss of thermoluminescence even at room temperature, which is well below the temperature of the main glow

peak.

Stored thermoluminescent energy decays less than 5% per year at room temperature and less than 15% per year at body temperature (Cameron et al., 1964). Another investigation (Suntharalingam et al., 1968) supported this finding. The loss of response was reported as less than 5% for a twelve week period at room temperature. This establishes that lithium fluoride shows a negligible decay of thermoluminescence if the response is measured soon after irradiation.

3.6 Dose Rate Dependence

Lithium fluoride has shown no dependence on dose rate from 5×10^2 to 2×10^{11} rads/second. This dose rate independence was first established in the range from 5×10^2 to 2×10^8 rads/second (Karzmark et al., 1964) and was later extended to 2×10^{11} rads/second by using flash X-ray units (Tochilin and Goldstein, 1966).

3.7 Measurement of Various Quality Radiation

Lithium fluoride dosimeters have been used to detect alpha particles (Jones et al., 1966), beta particles (Kastner et al., 1967), and X- and gamma rays (Cameron et al., 1968), protons (Parker et al., 1968), and neutrons (Wingate et al., 1967). The only radiations involved in this study were neutrons, high energy electrons, and X-rays; so the other types of radiation will not be discussed.

There is a possible problem with neutron contamination associated with high energy X-ray radiation. Fast, inter-

mediate, and slow neutrons will be produced through the photonuclear process (γ, n) in which the high energy X-ray is incident on the target material. The neutron yield is directly proportional to the X-ray energy and intensity, and is dependent on the target material. The extent of neutron contamination must be determined before the response of lithium fluoride to high energy X-rays can be accurately determined.

For the thermal neutrons, the $^{6}Li(n,\alpha)^{3}H$ reaction has a high cross section, about 950 barns. The alpha particle and triton release a total of 4.8 Mev of local ionizing energy. As a result of this reaction, TLD-100 dosimeters show a response to thermal neutrons.

On the basis of energy absorbed, thermal neutrons produce about one-seventh the amount of thermoluminescence produced by gamma rays in TLD-100 (Cameron et al., 1968). This can be explained by two effects: recombination of ionized particles along the densely ionized track, and saturation of the available trapping centers along the track.

TLD-700 contains almost entirely lithium-7 and has essentially no response to thermal neutrons. This is due to an extremely small neutron cross section. The response of TLD-700 to thermal neutrons has been found to be less than 0.5% of the response of TLD-100 (Cameron et al., 1964). Therefore, it essentially measures the photon dose in a mixed field of neutrons and photons.

The fast neutron response of lithium fluoride is not

dependent on isotopic composition as in the thermal neutron case. This is because its response is due primarily to lithium and fluorine ion knock-ons (Isotopes/Con-Rad, 1968a). The thermoluminescence from lithium fluoride TLD-100 or TLD-700 which have been exposed to 10^8 fast neutrons per cm^2 (about 1 rem), is less than the thermoluminescence from an exposure of 1 roentgen of photons (Cameron et al., 1964).

Thus, if a mixed field of photons and neutrons is present, the dose contribution from each can be measured by irradiating TLD-100 in combination with TLD-700 to the same field. The TLD-700 gives essentially the photon component, which is subtracted from the TLD-100 reading to obtain the thermal neutron component. Corrections must be made, however, for isotopic compositions in each type of material.

3.8 Range of Exposures

For lithium fluoride TLD-100, the relationship between thermoluminescence and exposure is linear up to about 10^3 roentgens. Above this, it becomes supralinear, that is thermoluminescence increases faster than proportionally to exposure. At about 5×10^5 roentgens, thermoluminescence reaches a maximum and decreases with increasing exposure (Cameron et al., 1964; Suntharalingam and Cameron, 1969). This relationship is shown in Figure 3.

The dose-response relationship for lithium fluoride TLD-700 is not as well established. One investigation found that TLD-700 had a response similar to that of TLD-100, and

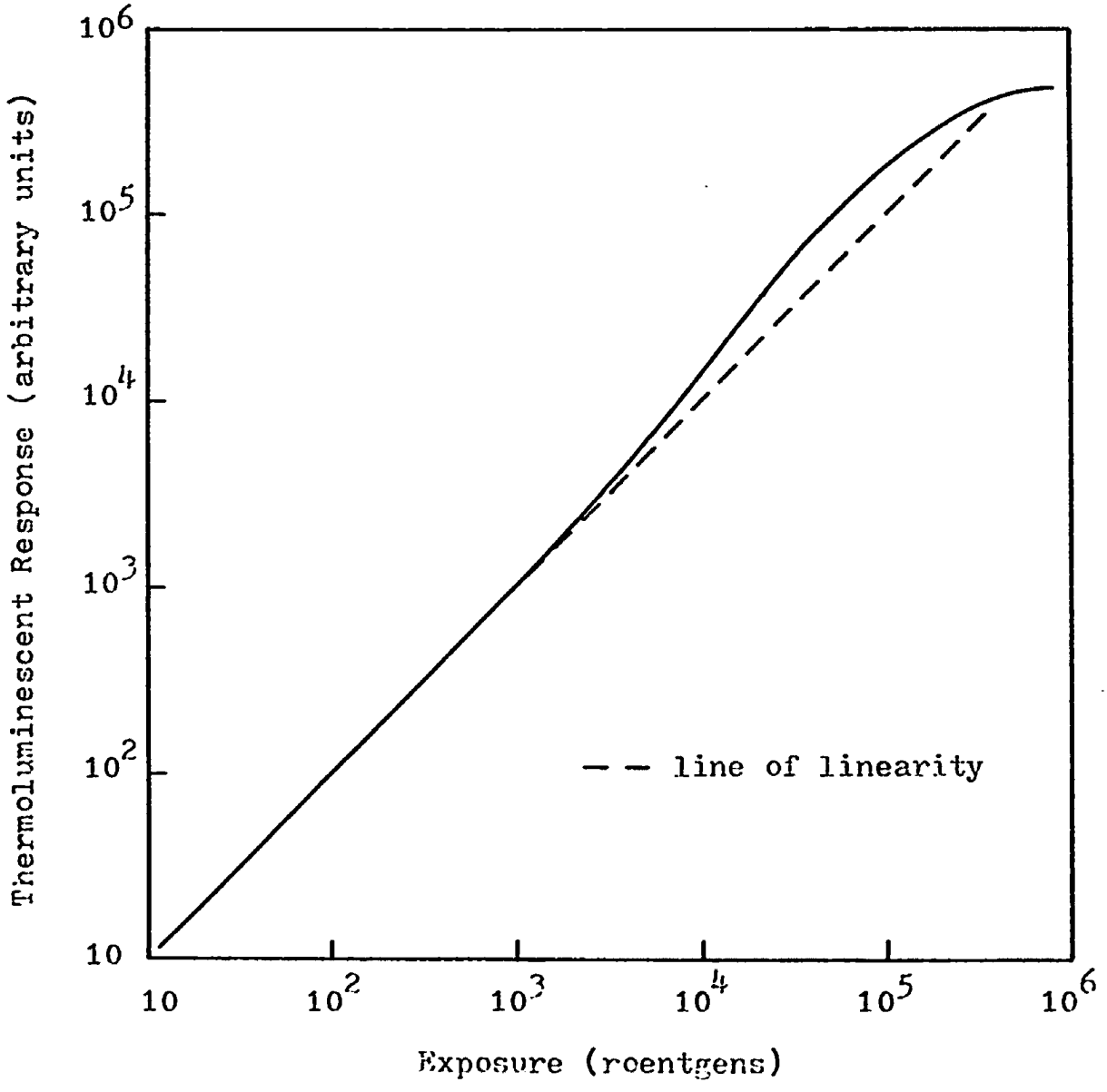

Figure 3. Exposure-Response Curve of Lithium Fluoride TLD-100. (Cameron et al., 1964)

that the response per rad dose changed less than 0.1% over the 50 to 1500 rad dose range (Pinkerton et al., 1967). Another investigation showed that in the 200 to 1400 rad dose range, the dose-response curve is a linearily increasing function, and the response increases about 17% from 200 to 1000 rads (Almond et al., 1967).

Supralinearity has also been noticed for TLD-700 and its magnitude is greater than for TLD-100. The point at which this supralinearity becomes apparent was found to be 500 rads (Suntharalingam and Cameron, 1969). Certain individual batches of TLD-700, however, have shown supralinearity as low as 200 rads (Almond, 1966).

Although the cause for supralinearity has not been well established, several models have been proposed (Cameron and Zimmerman, 1965; 1966; Cameron et al., 1967; 1967a; Suntharalingam, 1968). In these works, three possible causes for supralinearity have been mentioned: (1) the creation of additional trapping sites, (2) the creation of additional recombination centers, and (3) an increase in thermoluminescent efficiency. These models have been fit to experimental data, and the agreement is very good considering that the exact physical mechanism for supralinearity has not been established.

The plateau in Figure 3 can be explained by relating the number of filled traps to the total number of traps. Saturation is reached when the number of filled traps is a

significant fraction of the total number of traps. At this point, an increase in dose will create a proportional increase in electron-hole pairs, but they recombine immediately since there is a deficiency of trapping sites.

3.9 Thermoluminescent Response Below 1.2 Mev

It was first reported by Morehead and Daniels (1957) that the thermoluminescent response of lithium fluoride was dependent on the quality of radiation. They observed that the energy initially required to produce an F center (the specific site consisting of an ionized electron trapped by a fluoride ion vacancy) varied. It was about 700 ev for 2 Mev alpha particles, 140 ev for 2 Mev electrons, and 65 ev for both cobalt-60 gamma rays and thermal neutrons.

The total thermoluminescence observed after irradiation by alpha particles was less than that observed from the other radiations. For example, it took about 10 times greater exposure to alpha particles to produce the same thermoluminescent response as for the other radiations. This effect can be explained by high LET radiations being less effective in filling the available traps or activating the impurity sites (Suntharalingam, 1968; Suntharalingam and Cameron, 1969).

Numerous investigations were made on the thermoluminescent response of lithium fluoride during the ten years following Morehead and Daniel's work. These generally studied the energy range below cobalt-60 gamma rays, and can be characterized by the work of Cameron et al. (1964). They found

that the thermoluminescent response of lithium fluoride TLD-100 was about 25% greater at 30 kev effective than at 1.2 Mev.

This enhanced response at low energies can be interpreted as a response to absorbed energy rather than to exposure. At energies less than 50 kev, the absorption of energy is primarily by the photoelectric process. The conversion from an exposure in roentgens to an absorbed dose in lithium fluoride is given by:

$$f = 0.869 \frac{(\mu_{en})_{LiF}}{(\mu_{en})_{air}}$$

In this equation, f is the conversion ratio from roentgens to rads and μ_{en} is the energy absorption coeficient. The constant (0.869) is a conversion factor for roentgens to rads in air (Johns, 1961). Since $(\mu_{en})_{LiF}$ is greater than $(\mu_{en})_{air}$ at energies less than 50 kev, there is a greater absorption of energy in lithium fluoride than in air. This results in a greater sensitivity for lithium fluoride at low energies.

At energies from 200 kev up to 3 Mev, absorption is primarily by the Compton process and all materials absorb about the same amount per electron regardless of the atomic number (Johns, 1961). Therefore, the f conversion factor in this energy range will approach unity.

Figure 4 shows the calculated ratio between the mass energy absorption coefficients for lithium fluoride and air, as well as the measured data (Cameron et al., 1964) for the

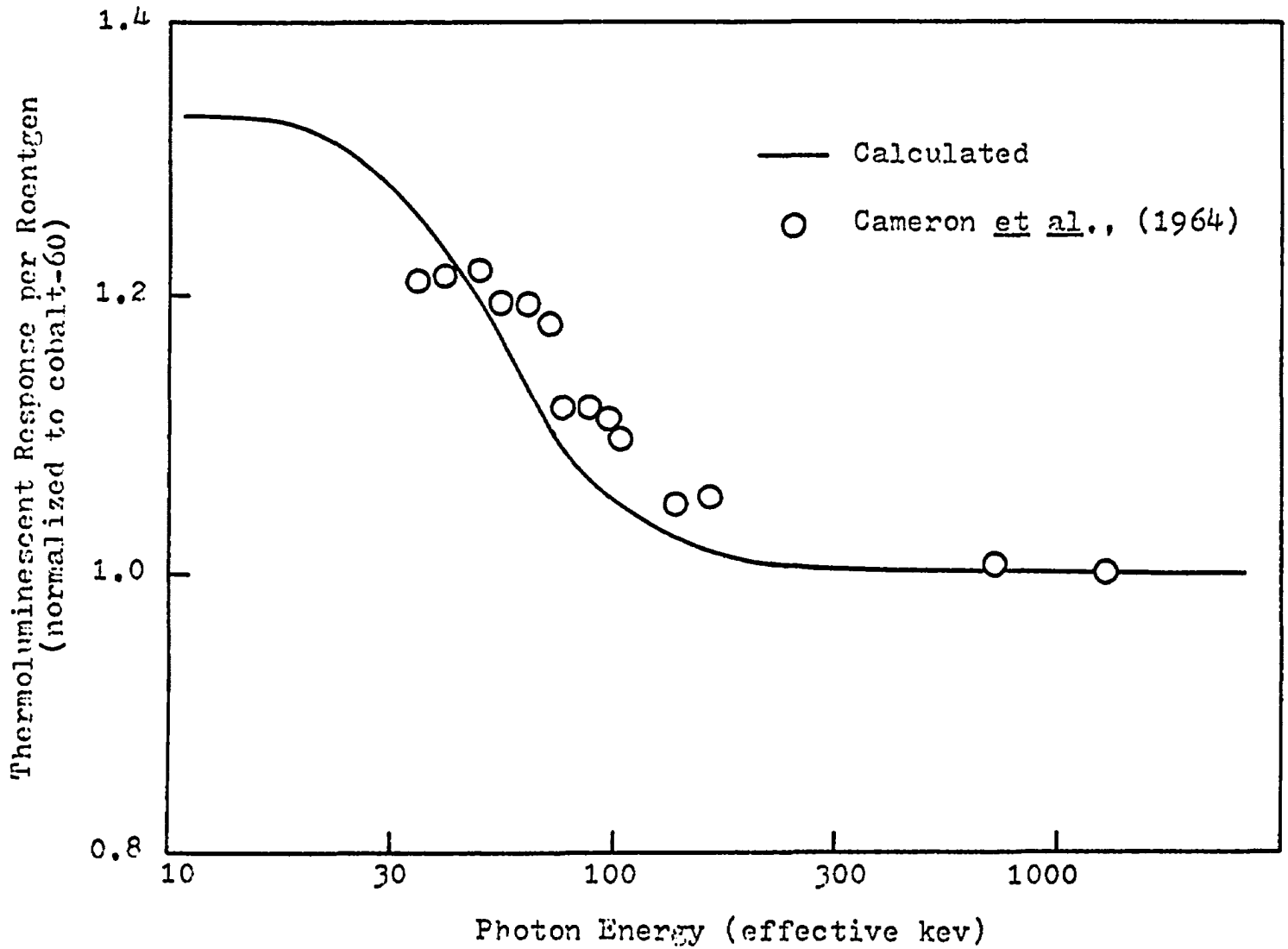

Figure 4. Calculated and Measured Thermoluminescent Response of Lithium Fluoride TLD-100 Below 1.2 Mev.

response of lithium fluoride per roentgen of exposure.

Another type of energy dependence that depends on the total dose of irradiation has been described (Naylor, 1965; Wagner and Cameron, 1966). It was found in TLD-100 that the dose-response relationship was energy dependent in the supralinear region, with the magnitude of supralinearity dependent upon the quality of radiation. Curves representative of this observation are shown in Figure 5. All curves are identical up to about 10^3 rads, because in the linear region lithium fluoride responds only to the amount of energy absorbed. In the supralinear region, however, a greater response is observed with lower LET radiations.

A model proposed to explain this effect assumes that supralinearity is caused by the creation of additional traps, and the efficiency of forming such traps is dependent on the quality of radiation (Worton and Holloway, 1966). A lithium fluoride dosimeter contains a certain number of sites capable of trapping electrons, and radiation is capable of not only filling these traps, but also of creating additional trapping sites. At low doses, the number of traps created would be small compared to those already present in the dosimeter, and therefore a linear response would be expected. At higher doses, if the creation of traps exceeds the filling of traps, the dose response curve would be expected to rise.

From this model, it appears that the ability to create traps increases with increasing energy, and the dose-response

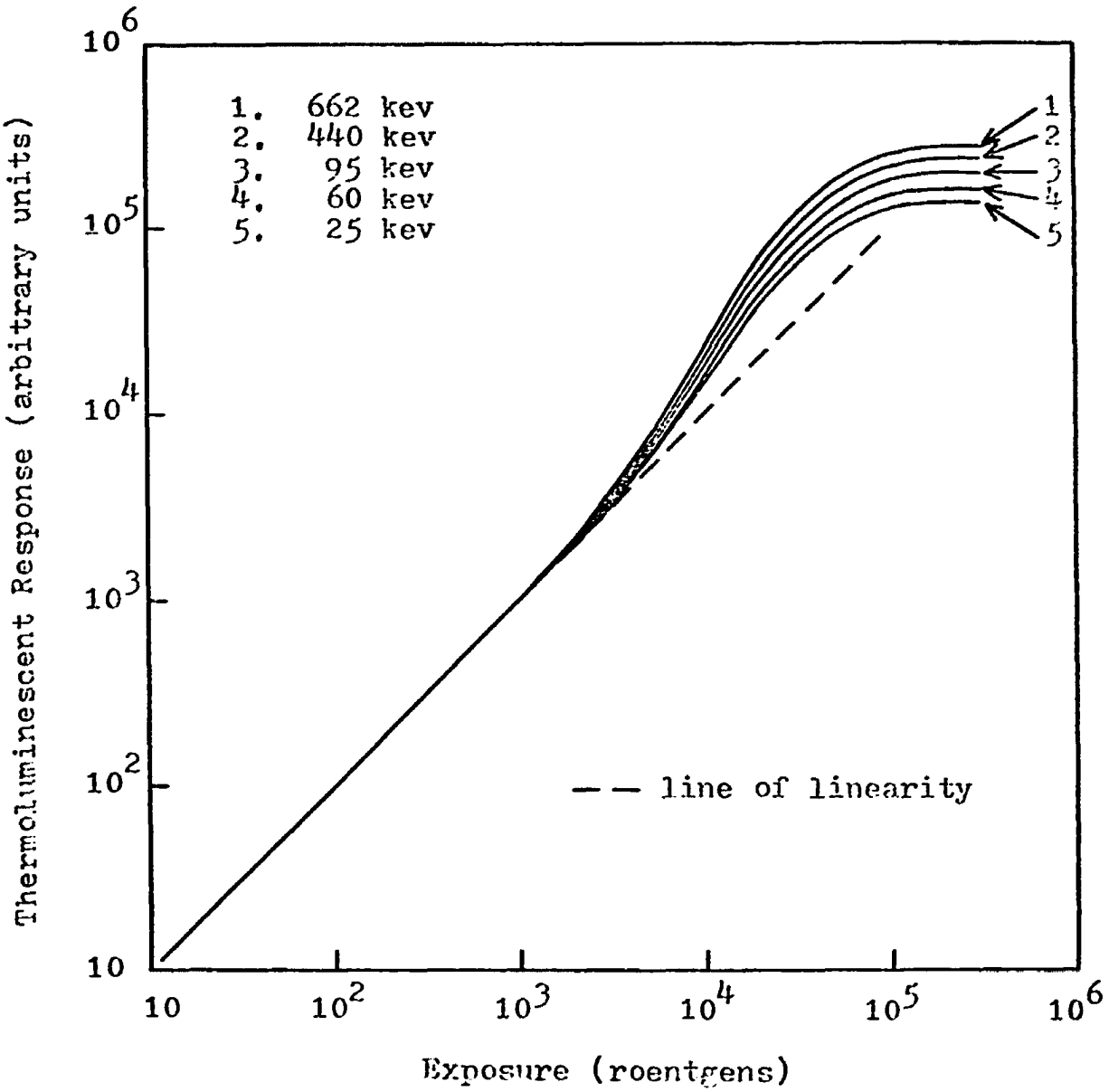

Figure 5. Exposure-Response Curve of Lithium Fluoride TLD-100 for Various Photon Energies. (Wagner and Cameron, 1966)

relationship shows a greater supralinearity at higher energies. This is because a lower ion-pair density is more effective in the creation of additional trapping sites since the energy is distributed over a larger volume and the probability of electron-hole recombination will be less (Wagner and Cameron, 1966). Thus, as effective energy increases, linear energy transfer will decrease and the greater will be the amount of supralinearity.

3.10 Thermoluminescent Response Above 1.2 Mev

During an intercomparison study among several installations on absorbed dose measurements, persistent differences in thermoluminescent response per rad in water were noticed between cobalt-60 gamma rays and high energy electron radiation (Pinkerton et al., 1967). The response to cobalt-60 was significantly greater than to high energy electrons of equal dose. Since this was contrary to the accepted idea of a flat response in the high energy region, it was decided to further investigate the effect of energy on the response of lithium fluoride.

Further investigations showed that lithium fluoride Type 7 (manufactured by Con-Rad and similar in composition to TLD-700) responded about 10% higher to cobalt-60 than to high energy electrons (Pinkerton et al., 1966). This relationship is shown in Table 1 and holds for both 10 Mev and 15 Mev electrons. The responses of both high energy electron radiations were not considered to be significantly different from

Table 1. Values of Thermoluminescent Response per Rad Normalized to Cobalt-60 for High Energy Electrons and X-rays.

Radiation	Pinkerton et al. 1966	Crosby et al. 1966	Benner et al. 1967	Nakajima et al. 1968
Cs-137		1.000±0.010		
Co-60	1.000	1.000	1.000	1.000
Electrons				
6 Mev		0.931±0.008		
9 Mev				
10 Mev	0.876±0.021	0.925±0.012		1.00±0.01
12 Mev				
15 Mev	0.893±0.018	0.903±0.021	0.94±0.05	1.01±0.03
18 Mev		0.886±0.015		
20 Mev			0.91±0.05	1.02±0.03
25 Mev			0.93±0.05	1.03±0.02
30 Mev			0.92±0.05	1.02±0.03
33 Mev			0.89±0.05	
35 Mev				
X-rays				
18.5 Mev				
22 Mev		0.916±0.012		

Table 1. (continued)

Radiation	Binks 1969		Almond and McCray 1970	
	Type N	Type 7	Calculated	Measured
Cs-137			1.019	0.99
Co-60	1.000	1.000	1.000	1.00
Electrons				
6 Mev			0.936	0.94
9 Mev			0.928	
10 Mev	0.876±0.016	0.904±0.019		
12 Mev			0.927	0.93
15 Mev	0.866±0.007	0.852±0.020	0.926	0.92
18 Mev			0.927	0.89
20 Mev	0.874±0.010	0.898±0.021		
25 Mev	0.879±0.037	0.928±0.022		
30 Mev	0.880±0.010	0.916±0.031	0.930	
33 Mev				
35 Mev	0.868±0.021	0.916±0.024		
X-rays				
18.5 Mev			0.927	0.94
22 Mev			0.926	0.93

each other.

In order to see if factors other than energy accounted for this difference, glow curves were taken at the three energy levels. No qualitative difference between the glow curves was detected, only a quantitative difference between the two types of radiation was observed. A larger area under the cobalt-60 curve indicated a greater response.

Another investigation resulting from participation in the intercomparison study found a gradual decrease in the sensitivity of TLD-700 as the radiation energy was increased (Crosby et al., 1966). This result is also shown in Table 1, and generally agrees with the previous investigation. It found about a 10% decrease in sensitivity between cobalt-60 and 15 Mev electrons. There is, however, a significant decrease in sensitivity with increasing electron energy. This was reported as a rather unexpected result and no physical explanation was offered for this observation.

Others have studied this effect for lithium fluoride TLD-100, Type 7, and Type N (manufactured by Con-Rad and similar in composition to TLD-100) and their results are shown in Table 1 (Benner et al., 1967; Binks, 1969). They confirmed the previous investigation that showed about a 10% decrease in sensitivity from cobalt-60 to high energy electrons, but failed to find any significant change in sensitivity with increasing electron energy.

On the other hand, it was found that the response of

lithium fluoride Type 7 is dependent on electron energy (Almond et al., 1967). This dependence is shown in Figure 6, and indicates a significant decrease in sensitivity with increasing energy. This data does confirm, however, that lithium fluoride is about 10% less sensitive to 15 Mev electrons than to cobalt-60.

One investigation, however, failed to find any difference in thermoluminescent response between cobalt-60 and high energy electrons, or among various electron energies (Nakajima et al., 1968). The lithium fluoride used in this investigation was in crystalline form and supplied by the Institute for Applied Optics in Tokyo. The isotopic composition of this material was not given and the experimental design was different than the other investigations, so any comparison of this data (as shown in Table 1) and data from the investigations discussed previously would be difficult to interpret.

An interesting comparison has been developed between the measured and calculated sensitivities for lithium fluoride TLD-700 to cobalt-60 gamma rays, and high energy electrons and X-rays (Almond and McCray, 1970). As shown in Table 1, the measured response confirmed their previous investigations (Crosby et al., 1966; Almond et al., 1967) which showed about a 10% decrease in sensitivity to high energy electrons and X-rays as compared to cobalt-60, and a gradual decrease in sensitivity with increasing electron energy.

In order to explain these results, the expected responses

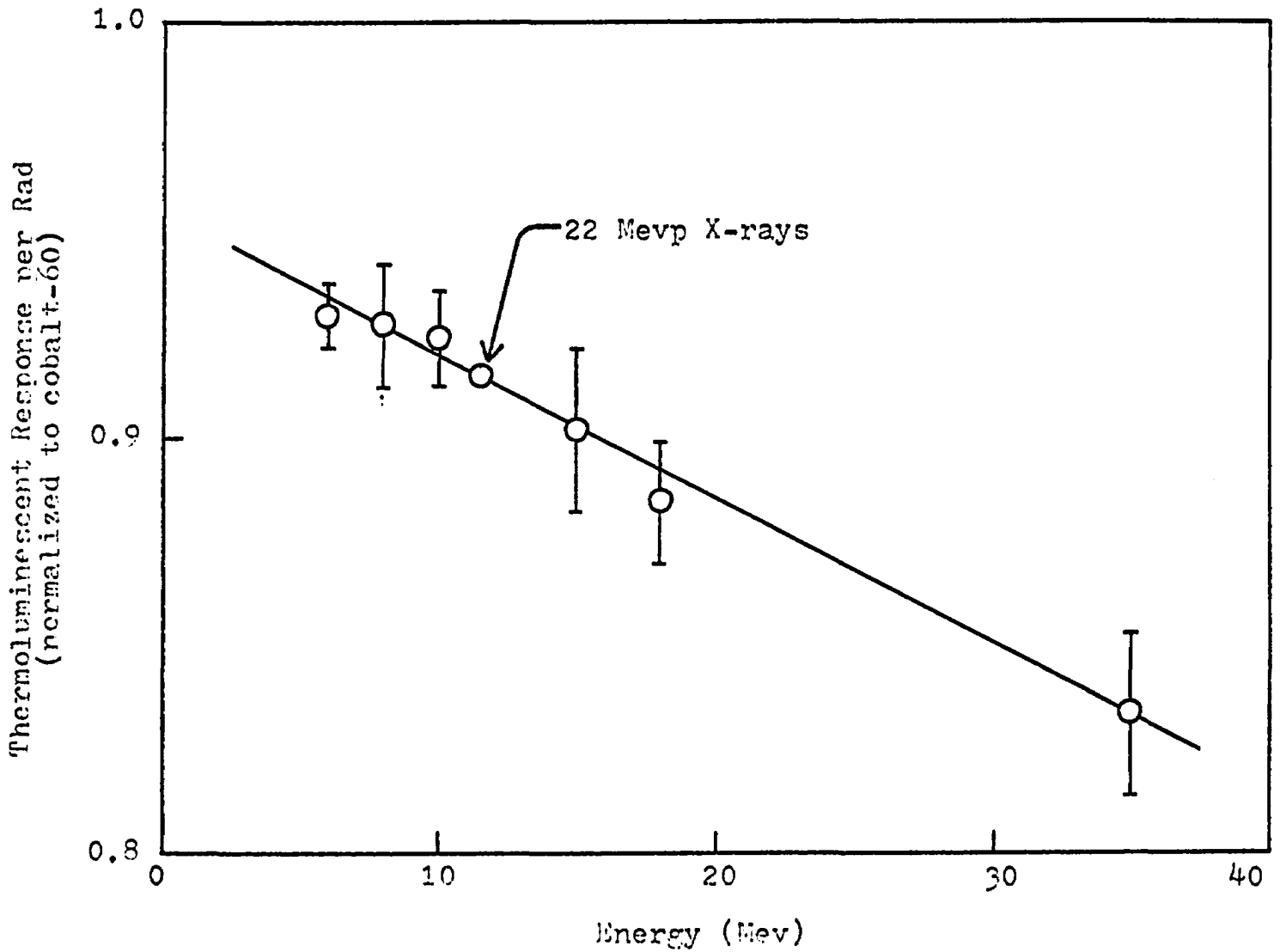

Figure 6. Thermoluminescent Response of Lithium Fluoride Con-Rad Type 7 for High Energy Electrons and X-rays. (Almond et al., 1967)

were calculated using the general cavity theory derived by Burlin (1966; 1968; Burlin and Chan, 1967). Almond and McCray did, however, extend the Burlin theory to include high energy electrons and X-rays.

Cavity theory is generally used to express the relationship between absorbed dose in a cavity and absorbed dose in the medium at the point of the cavity. The part of Burlin's general theory applicable to this problem considers the intermediate cavity sizes in which the cavity dimensions are comparable with the electron ranges. The electron spectrum within the cavity is neither completely determined by the medium nor by the cavity. Almond and McCray extended this theory to account for the attenuation of the electron spectrum from the medium, which is due to absorption within the medium itself, and the build-up of the electron spectrum in the cavity, which is due to photon interactions within the cavity.

Almond and McCray applied this extended theory to calculate the relative sensitivity of lithium fluoride to high energy electrons and X-rays as compared to cobalt-60 gamma rays. Relative sensitivity was taken as the thermoluminescent response per rad at the energy of interest normalized to the thermoluminescent response per rad for cobalt-60 gamma rays.

The sensitivities calculated from this theory predict that the response of lithium fluoride as compared to cobalt-

60 will decrease with increasing energy. There is good agreement between the calculated and measured points as shown in Table 1. It appears that this theory explains well the apparent decrease in sensitivity reported for lithium fluoride. Therefore, the observed decrease in sensitivity is due to a decrease in absorbed dose with increasing energy rather than to an energy dependence of lithium fluoride. It was concluded that lithium fluoride thermoluminescence shows no energy dependence.

Details of experimental conditions were not consistent among any of the investigations mentioned so far in this section, and their results can not be directly compared. With one exception, there is general agreement that lithium fluoride responds less to high energy electrons and X-rays than to an equivalent dose from cobalt-60. If this response is real, it is reasonable to expect close agreement among independent investigations since all measurements were made in the dose range between 100 and 300 rads. This is below the region of supralinearity. No report, however, offered any physical explanation for this response.

An explanation has been offered, however, to explain the lack of dependence of thermoluminescent response on energy that several investigators have reported (Suntharalingam, 1968). Thermoluminescent response is proportional to the amount of energy deposited within the dosimeter material, and stopping power provides a means for expressing the mean energy loss per unit path length in matter.

Stopping power values as a function of energy show a broad minimum from about 400 kev to 20 Mev, and gradually increase with energy above 20 Mev (Berger and Seltzer, 1964). Any small changes in stopping power in the neighborhood of the broad minimum would be insufficient to justify any significant change in thermoluminescent response.

The energy dependence of the dose-response relationship for lithium fluoride has also been studied for high energy electrons and X-rays. There is little agreement among the investigators who have measured this response.

One investigator measured the thermoluminescent response of lithium fluoride Type 7 to both cobalt-60 gamma rays and 15 Mev electrons (Almond et al., 1967). In the dose range between 200 rads and 1400 rads, thermoluminescent response per rad was observed to be a linearily increasing function for both types of radiation (see Figure 7). It has been suggested that the increased sensitivity with increasing dose is due to the creation of additional trapping sites (Naylor, 1965). Since the curves for cobalt-60 and 15 Mev electrons are parallel, the efficiency of forming such traps must be the same for both qualities of radiation.

Another investigator used lithium fluoride Type N in the 10 rad to over 10^3 rad range (Worton and Holloway, 1966). As shown in Figure 8, it was also determined that the response was a function of the dose measured, but that it became greater with larger doses. But unlike other reports, the response

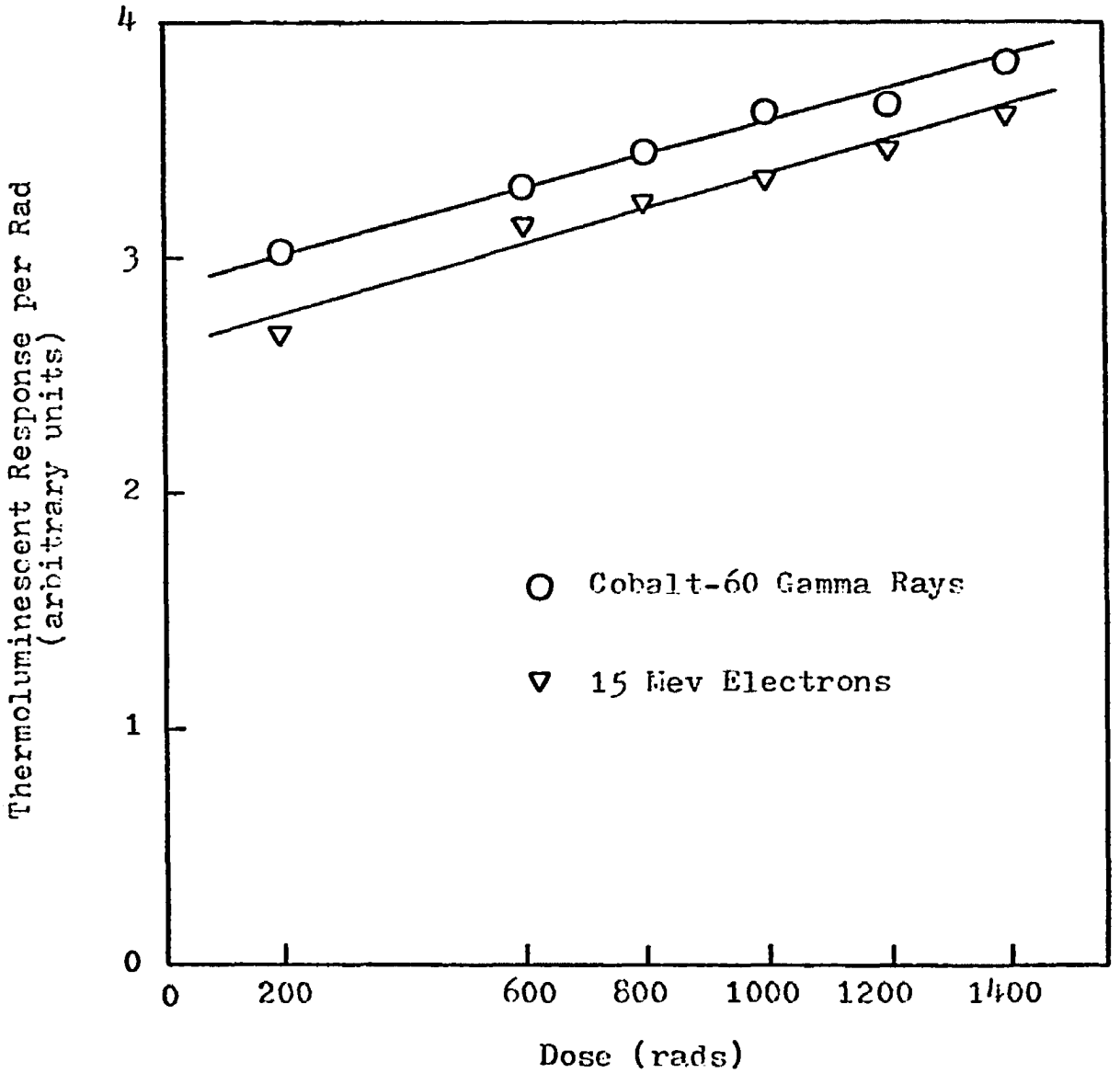

Figure 7. Dose-Response Curve of Lithium Fluoride Con-Rad Type 7 for Cobalt-60 Gamma Rays and 15 Mev Electrons. (Almond et al., 1967)

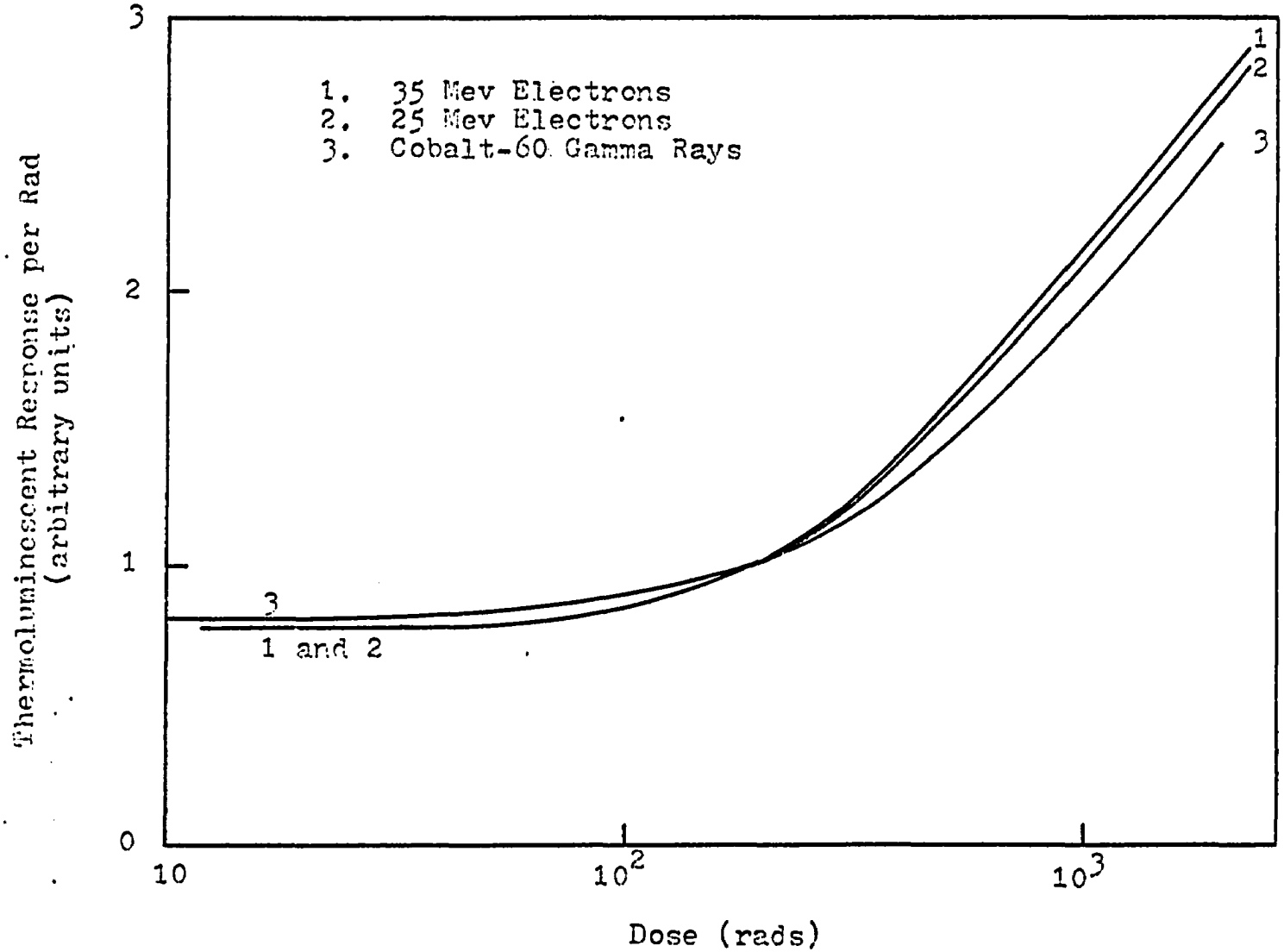

Figure 8. Dose-Response Curve of Lithium Fluoride Con-Ray Type N for Cobalt-60 Gamma Rays, 25 Mev Electrons, and 35 Mev Electrons. (Worton and Holloway, 1966)

per rad rises more sharply for the high energy electron radiations than for cobalt-60. A discussion of the model to explain this result was presented in section 3.9.

Two additional studies also found that supralinearity in lithium fluoride TLD-100 was dose dependent, but found no difference in response between cobalt-60 and high energy electrons throughout a wide dose range (Suntharalingam and Cameron, 1969; Ehrligh, 1970). This relationship is shown in Figure 9. A model for this result has also been proposed based on stopping power, and was discussed earlier in this section (Suntharalingam, 1968).

These studies demonstrate the lack of consistency among the investigations on the effect of the quality of radiation on the dose-response relationship and the models proposed to explain these results. This effect appears to be significant, especially at higher doses, and must be more accurately defined before measurements can be made with any degree of certainty.

The errors reported in these works represent only the standard deviations of the thermoluminescent readouts. They do not include an allowance for the overall error in experimental design. If the overall error had been considered, the significance of some of these results might be questionable.

All studies reported in this chapter used lithium fluoride in powder form. In addition, Ehrligh (1970) used lithium fluoride TLD-100 plaques 0.25 in. x 0.25 in. x 0.035 in.

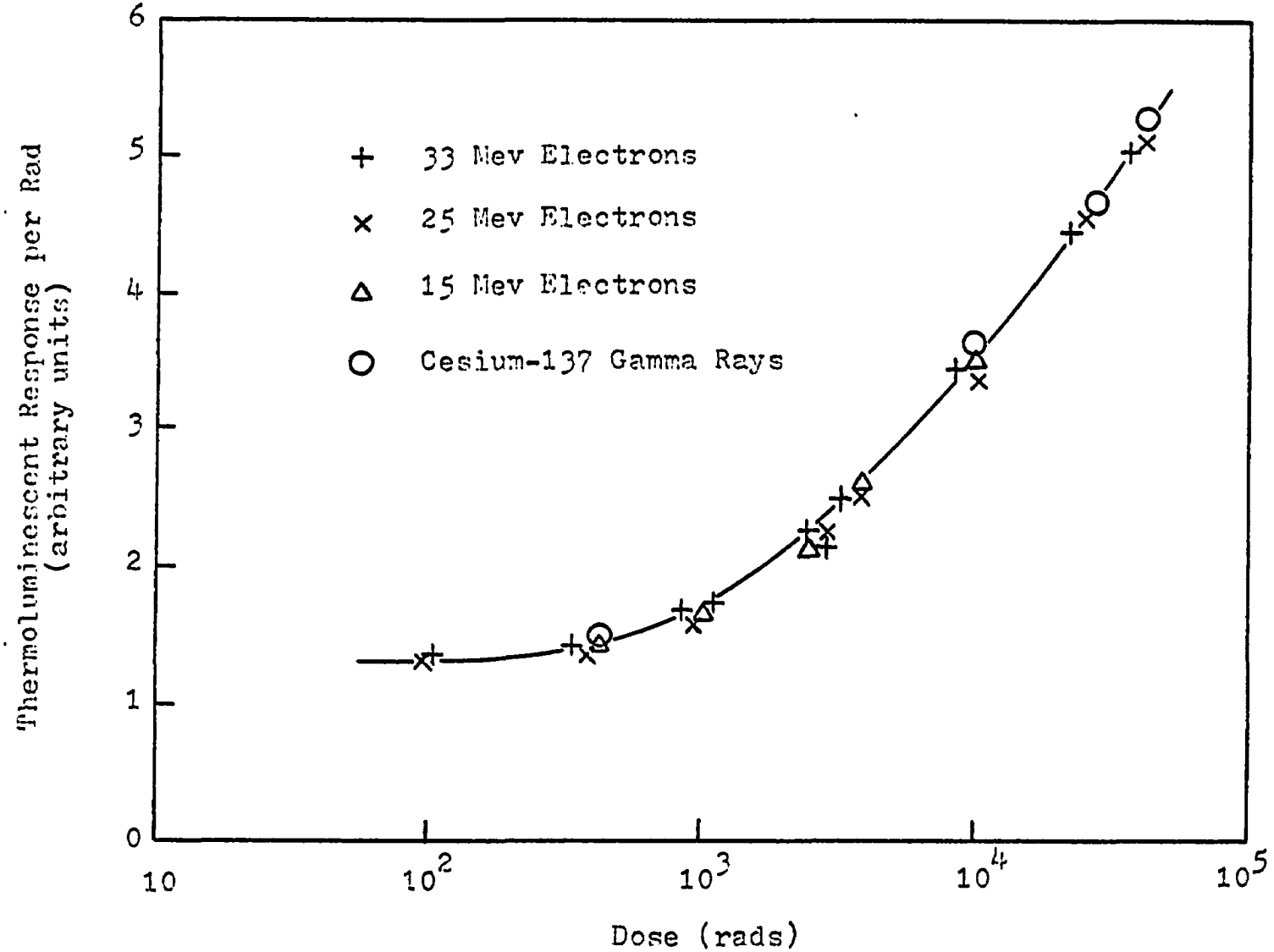

Figure 9. Dose-Response Curve of Lithium Fluoride TLD-100 for Cesium-137 Gamma Rays, 15 Mev Electrons, 25 Mev Electrons, and 33 Mev Electrons. (Suntharalingam and Cameron, 1969)

and found the response of this form to be similar to lithium fluoride TLD-100 powder.

The lack of agreement among the results of these investigations could be due to the configuration of the phosphor. Since this was not reported by most investigators, a comparison of results based on dosimeter configuration could not be made.

CHAPTER IV

ABSORBED DOSE

4.1 Measurement

The measurement of absorbed dose was made by placing a dosimeter within the material of interest and on the central axis of the incident photon beam. This dosimeter records in its sensitive volume the energy deposited by secondary electrons produced by the photon beam. These electrons may be produced within the dosimeter itself, within the surrounding material, or outside the material of interest. To correctly interpret such a measurement complete information is needed on the origin of all electrons interacting with the dosimeter. Although many authors have presented a discussion of absorbed dose, the reader is referred to Johns (1961) for a detailed presentation.

The absorbed dose at any point in the material of interest is usually expressed as a percent of the maximum value of the absorbed dose which occurs along the central axis of the incident beam (ICRU, 1962). A plot of this function is called the depth-dose distribution and is shown in Figure 10.

Curve A represents the depth-dose distribution where only the secondary electrons produced in the material of interest, or within the dosimeter itself, are considered. This type of distribution is generally obtained when the incident photon beam is free of secondary electrons.

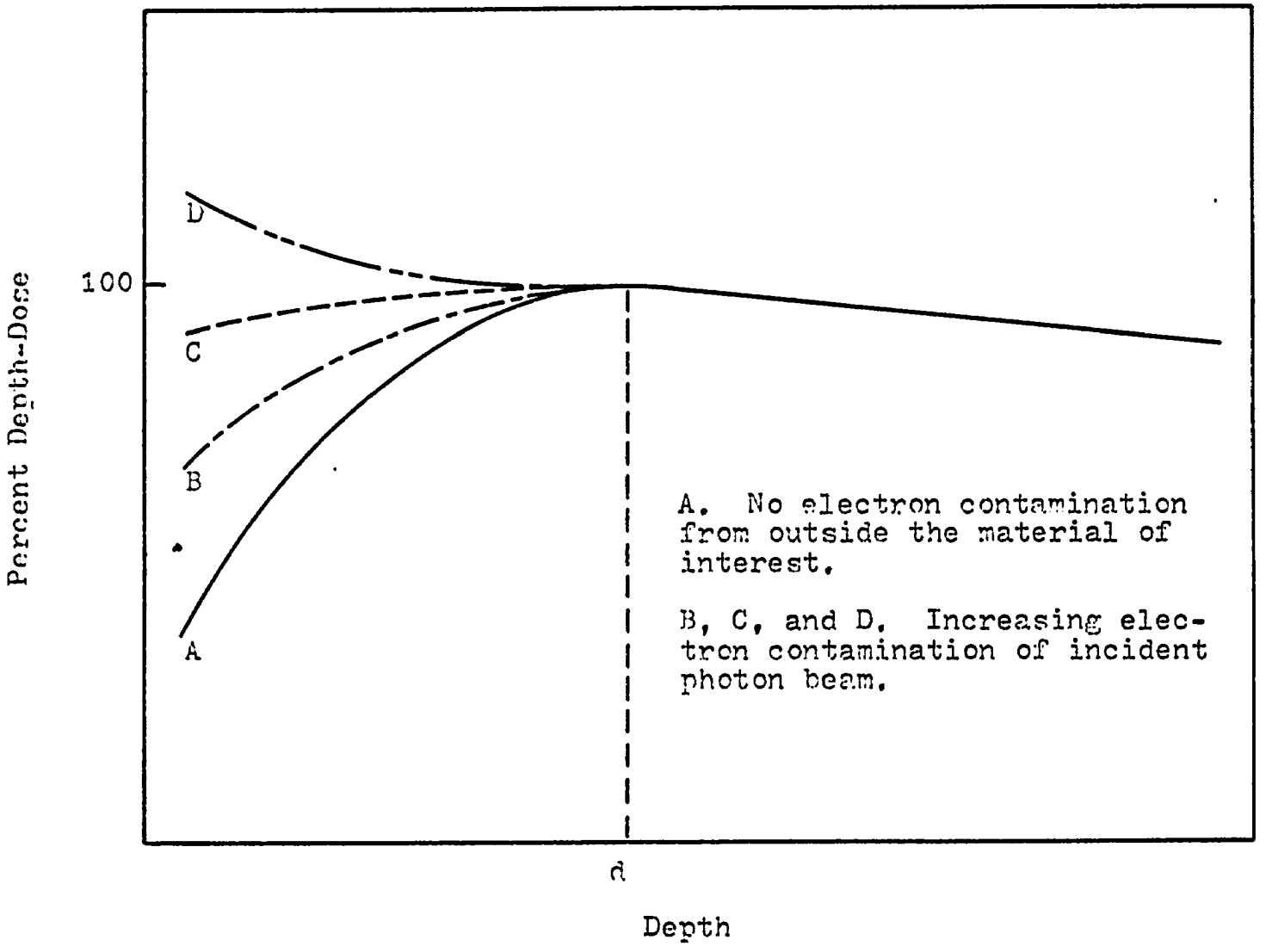

Figure 10. Relative Depth-Dose Distribution. (Wyckoff, 1967)

The initial buildup with depth is due to the gradual establishment of conditions approaching electronic equilibrium, even though this situation is not actually attained. Absorbed dose will increase to a maximum at d, which is at a depth less than the maximum electron range in the material. This is due to the range of the electrons being comparable to the photon range. In these distances, attenuation is appreciable. Beyond the peak dose, the curve will fall exponentially due to attenuation of the incident photon beam in the material.

In practice, however, this distribution is difficult to attain. The dose-distribution will depend not only on the incident photon beam, but also on any secondary electrons arising from outside the material. Extraneous objects, like beam defining collimators, filters, etc., close to the surface of the material will contribute to the production of these secondary electrons. They may accompany the incident photon beam into the material to about the peak dose depth.

Curves B, C, and D result from differnt amounts and energies of electron contamination of the incident photon beam. Beyond the depth d, all curves coincide. Thus, a depth of d or greater was used for all measurements in this study. Any measurements taken at depths less than d, will depend on the individual photon source and experimental design, and there is no common basis for normalization if results are to be compared from various installations.

4.2 Cavity Theory

The measurement of absorbed dose necessitates the insertion of a dosimeter into the medium under investigation. The dosimeter usually differs in both atomic number and density from the medium and will therefore constitute a discontinuity in the medium. Under these conditions the dosimeter can be referred to as a cavity.

Cavity theory is concerned with the relationship between absorbed dose in the medium and absorbed dose in the dosimeter or cavity. Absorbed dose as measured by the dosimeter is a function of photon energy and dosimeter size and composition. To relate this measurement to an absorbed dose in the medium, the composition of the medium must also be considered.

A general cavity theory for X-rays has been derived by Burlin (1966; 1968; Burlin and Chan, 1967; 1970). Where facts in the discussion of this theory are not referenced, a through review can be found in these references.

An equation expressing the relationship between absorbed dose in the medium, D_m, and the absorbed dose in the cavity, D_c, is:

$$D_m = \frac{1}{f} D_c$$

where f is the conversion factor between D_m and D_c.

In order to investigate the limits of the conversion factor, consider an X-ray beam passing through a medium. The photons interact with electrons, producing ionization. This

occurs in both medium and cavity material.

If the cavity dimensions are large compared with the electron ranges, the absorbed dose contribution is negligible from electrons generated within the medium. The electron spectrum in the cavity will therefore be determined by the cavity. Absorbed dose within the cavity itself will be independent of the surrounding material. The absorbed dose will be proportional to the mass energy absorption coefficient of the cavity $(\mu_{en}/\rho)c$.

The absorbed dose in the medium will be proportional to the mass energy absorption coefficient for the medium $(\mu_{en}/\rho)m$. Absorbed dose in the medium can then be related to absorbed dose in the cavity through the correction factor f.

$$f = \frac{(\mu_{en}/\rho)c}{(\mu_{en}/\rho)m}$$

Values for mass energy absorption coefficients have been determined by Hubbell (1969) and Evans (1968). This relationship is valid only when the presence of the cavity does not disturb the photon flux through the medium. If this condition is not met, a factor must be introduced into the equation to account for this effect.

On the other hand, if the cavity dimensions are small compared with the electron ranges, photon interactions generating electrons in the cavity are negligible, and the electron spectrum established in the medium is not disturbed

by the presence of the cavity. Therefore, the electron spectrum within the cavity will be determined by the medium.

To express the ratio between absorbed dose in the medium and absorbed dose in the cavity, an expression must be determined for the electron spectrum developed in the medium by photon interactions, and the rate at which these electrons lose energy per unit path length as they traverse the two materials. This has been expressed as the mass stopping power ratio for the electrons of the cavity to the medium.

$$f = \frac{1}{S_c^m}$$

Values for mass stopping power have been determined by Berger and Seltzer (1964).

In his general cavity theory Burlin also considers cavity dimensions comparable with the electron ranges. In this case, Burlin has developed the theory to account for conditions in-between the two extremes mentioned earlier.

For an intermediate size cavity, the basic assumptions for the extreme cases no longer hold. First of all, the electron spectrum set up in the medium is now significantly attenuated across the cavity. The energy distribution of the spectrum changes little during absorption, and is generally assumed to be constant across the cavity. The electron spectrum is attenuated on the average by a factor, d, which is determined from the following expression.

$$\frac{\int_o^g e^{-\beta x}\, dx}{\int_o^g dx} = \frac{1 - e^{-\beta g}}{\beta g} = d$$

β is the effective mass absorption coefficient of the electrons in the cavity and g is the average path length of the electrons in crossing the cavity.

The second assumption violated in this intermediate case results from photons generating electrons in significant amounts within the cavity. Since the resulting electron spectrum will have the same energy distribution as generated in the medium, Burlin has shown this to be a corollary of the previous case. Therefore, the spectrum generated in the cavity on the average builds up to (1 - d) of its equilibrium value.

$$\frac{\int_0^g (1 - e^{-\beta x})dx}{\int_0^g dx} = (1 - d)$$

The expression for d is applicable only when the cavity density is unity. Cavity materials with densities different than unity can be considered by replacing the effective mass absorption coefficient with the effective linear absorption coefficient. The effective linear absorption coefficient is calculated by multiplying the effective mass absorption coefficient by the density of the cavity material, i.e. $\beta\rho$. Considering cavity density, Burlin's expression for d becomes:

$$d = \frac{\int_0^g e^{-\beta\rho x}dx}{\int_0^g dx} = \frac{1 - e^{-\beta\rho g}}{\beta\rho g}$$

where $\beta\rho g$ is dimensionless.

Almond and McCray (1970) have followed Burlin's cavity theory and have arrived at a usable expression for the cor-

rection factor, f. They considered the partial attenuation of the electron spectrum from the medium in the cavity and the partial buildup of the electron spectrum in the cavity due to photon interactions in the cavity. Their expression is:

$$f = d \frac{1}{S_c^m} + (1 - d) \frac{(\mu_{en}/\rho)_c}{(\mu_{en}/\rho)_m}$$

If the cavity is very large, d approaches zero and the expression reduces to the ratio of mass energy absorption coefficients. If the cavity is very small, d approaches unity and the expression becomes the mass stopping power ratio.

In calculating the factor, d, Almond and McCray determined the effective mass absorption coefficient, β, from the following expression:

$$\beta\,(cm^2/gm) = \frac{17}{E^{1.14}}$$

where E is the maximum energy, in Mev, present in the electron spectrum.

It is therefore concluded that the correction factor, f, for the intermediate case be used to establish the ratio of absorbed dose in the medium to absorbed dose in the cavity. The built-in weight factor, d, will correct for any extreme situations. It should be noted that cavity configuration is as important as photon energy and atomic composition of both cavity and medium. The correction

factor, f, is dependent on all three.

4.3 Calibration Standard

The response of the ferrous sulfate, or Fricke, dosimeter to ionizing radiation was first described by Fricke and Morse (1927). Since then, it has been extensively studied and its response has been well established. This dosimeter is now used for the precision measurement of absorbed dose.

Recently, much effort has been invested in describing its response to high energy photons and electrons. As a result, the ferrous sulfate dosimeter is widely used for absorbed dose standardization for these radiations.

An up-to-date comprehensive review of chemical dosimetry has been presented by Spinks and Woods (1964) and Fricke and Hart (1966); and a thorough discussion can be found in these references. For the purpose of this study, however, only a brief review of the mechanisms involved in ferrous sulfate dosimetry will be presented. A summary of this nature has also been presented by Broszkiewicz (1967).

Ferrous sulfate dosimetry involves the oxidation of ferrous ions to ferric ions in a dilute aqueous solution. Irradiation of this system gives rise to free radicals and molecular products. Hydrogen atoms (H), hydroxyl radicals (OH), hydroperoxy radicals (HO_2), and hydrated electrons (e^-_{aq}) constitute the free radical group while

hydrogen (H_2) and hydrogen peroxide (H_2O_2) constitute the molecular product group. Hydrogen atoms and hydroxyl radicals are the active species initially formed by the dissociation of water during irradiation and are located along the tracks of the ionizing radiations. All other products are formed during the diffusion of the active products away from the tracks.

The chemical reactions oxidizing ferrous ions to ferric ions in a dilute aqueous solution involve the free radicals and molecules mentioned above. The simplified reactions proposed for this oxidation are:

$$H^+ + OH^- \xleftarrow{\text{Ionizing Radiation}} H_2O \longrightarrow H + OH$$

$$Fe^{+2} + OH \longrightarrow Fe^{+3} + OH^-$$

$$H + O_2 \longrightarrow HO_2$$

$$Fe^{+2} + HO_2 \longrightarrow Fe^{+3} + HO_2^-$$

$$HO_2^- + H^+ \longrightarrow H_2O_2$$

$$Fe^{+2} + H_2O_2 \longrightarrow Fe^{+3} + OH + OH^-$$

Each hydrogen atom forms a hydroperoxy radical which in turn leads to the oxidation of three ferrous ions. Each hydroxyl radical oxidizes one ferrous ion whereas each hydrogen peroxide molecule oxidizes two ferrous ions. The importance of the hydrated electron in this chemical reaction

is that it is quickly converted to a hydrogen radical (H) in acid solution.

The usefulness of this system in dosimetry is that the chemical change or amount of oxidation caused by irradiation is proportional to the absorbed dose. Therefore, a determination of the quantity of ferric ions produced by radiation can be related to absorbed dose. Since the radiation induced oxidation is irreversible, the concentration of ferric ions can be considered as a permanent measure of absorbed dose.

The yield for these oxidation reactions is expressed by a G value, where the value of G (Fe^{+3}) would indicate the number of ferric ions produced for each 100 ev of absorbed radiation energy. Unfortunately, this G value is dependent upon the linear energy transfer of the incident radiation. An increase in linear energy transfer will decrease the ferric ion yield. This is because the free radicals are formed closer together, and due to their high reactivity, they recombine before they can oxidize ferrous ions.

The recommended values of G (Fe^{+3}) for the ferrous sulfate dosimeter are 15.5 for cobalt-60 radiation, 15.6 for X-ray beams from 5 Mev to 10 Mev, and 15.7 for X-ray beams from 11 Mev to 30 Mev (ICRU, 1969). The temperature during irradiation should be between 20°C and 25°C in order to apply the G (Fe^{+3}) values. The values up to

10 Mev were derived from a survey of published measurements. At higher X-ray energies, the observations were too few and too inconsistent to define the yield factor based on experimental data. It had been predicted that the yield value for 25 Mev X-rays should be about 1% greater than that for cobalt-60 radiation (Burch, 1959) and it has been observed that numerous investigations of yield values were constant at 15.5 for electron radiations between 1 Mev and 30 Mev (Shalek and Smith, 1969). Both of these observations indicate that a value of about 15.7 is appropriate for X-ray beams from 11 Mev to 30 Mev.

At effective photon energies between 10 Mev and 100 Mev, a yield value of 15.6 has been proposed (Shalek and Smith, 1969). This value, although not supported by experimental data, was calculated from the gamma ray energy absorption data of Hubbell (1969). Figure 11 shows a plot of ferric ion yield as a function of photon energy as reviewed by Shalek and Smith (1969).

The standard solution for dosimetry consists of 0.001 M $FeSO_4$ and 0.001 M NaCl in air-saturated 0.8 N H_2SO_4. In this solution, the ferric ion yield is proportional to absorbed dose over a limited range. The upper level of about 4×10^4 rads is set by the oxygen content of the air-saturated aqueous solution. Above this value, the oxygen will be completely depleted. This stops the reaction between hydrogen atoms and oxygen which forms hydroperoxy radicals.

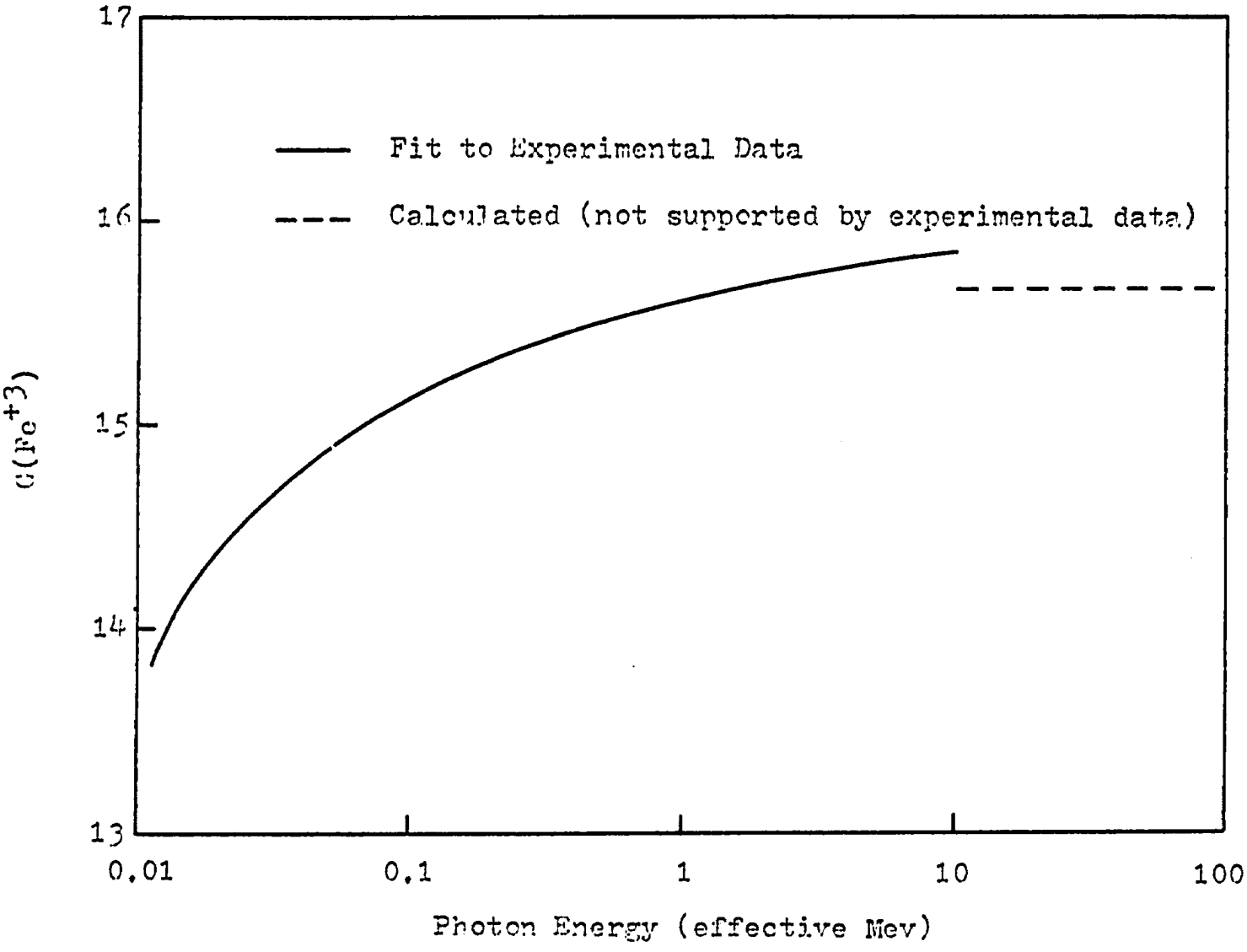

Figure 11. Yield of Ferric Ions per 100 ev in the Ferrous Sulfate Dosimeter as a Function of Photon Energy. (Shalek and Smith, 1969)

Stopping the yield of HO_2 will decrease the ferric ion yield.

The lower level of sensitivity is determined by the sensitivity of the analytical method used to detect ferric ion concentration and the presence of impurities in solution. The oxidation of ferrous ions is very sensitive to the presence of both organic and inorganic impurities. Inorganic impurities are less important and their control may be achieved by distillations of the aqueous solution.

Organic impurities, however, can influence the ferric ion concentration by reacting with hydrogen atoms and hydroxyl radicals to form organic radicals. This prevents the formation of the peroxides and hydroperoxides which initiate the chain oxidation of ferrous ions. This can reduce the ferric ion concentration to where it is no longer proportional to absorbed dose.

The NaCl is added to solution to reduce the effect of these organic impurities. The chlorine ions react rapidly with hydroxyl radicals

$$Cl^- + OH \longrightarrow Cl + OH^-$$

and the chlorine atoms formed, in turn, oxidize ferrous ions. This reaction is much faster than reactions with organic molecules.

Impurities may also be contributed by the irradiation vessel itself. For this reason, the vessels made for this study were constructed from teflon, which has been found to contribute negligible impurity levels. As a precaution

against organic impurity contamination, the new vessels were filled with ferrous sulfate solution and then irradiated to 15 megarads before being used for dosimetry purposes.

In the absence of radiation, aerated ferrous sulfate solutions slowly oxidize. This also affects the lower limit of dose which can be measured with accuracy. A correction for this oxidation can be obtained from an unirradiated sample of the same solution used as a control. A spontaneous dark oxidation exceeding this value indicates impurities.

The formation of ferric ions is directly proportional to energy absorbed between these limits as long as some oxygen remains in solution. Any deviation from proportionality indicates the exhaustion of dissolved oxygen and/or the presence of impurities. The formation of ferric ions has also been found to be independent of dose rate between 0.1 and 4,000 rads per second. The yield of ferric ions is little affected by temperature, and usually no correction is made for irradiations at or near room temperature (Shalek and Smith, 1969). The positive temperature coefficient at the time of irradiation is 0.04 ± 0.03 percent per degree C between 0°C and 70°C (Schwarz, 1954).

The ferric ion concentration was measured by direct spectrophotometric observations. In the dilute H_2SO_4 solution, practically all of the ferric ions are in the $FeSO_4^+$ form. This entity has absorption maxima at both 224 nm and 304 nm. Quantitative measurements are usually

made at the 304 nm peak since spectrophotometric adjustment is much more critical and impurities have a greater effect at the shorter wavelength. At the 304 nm wavelength, the molar extinction coefficient has been very precisely measured at 2,196 liters $mole^{-1}$ cm^{-1} at 25°C with a positive temperature coefficient of 0.69% per degree C (Scharf and Lee, 1962).

Once the ferric ion concentration has been determined, the average absorbed dose in rads in the ferrous sulfate solution can be determined. Shalek and Smith (1969) have developed a convenient formula for this calculation, and their method was used in this study.

CHAPTER V

EXPERIMENTAL DESIGN

5.1 Photon Source

The photon source used for this study was a 70 Mev synchrotron manufactured by General Electric Company and operated by the Department of Radiological Sciences of the University of Oklahoma Medical Center.

The synchrotron accelerates electrons in a circular orbit. An increasing magnetic field holds the electrons in orbit while an alternating electric field applied in synchronism with the orbital period provides the accelerating force. At the end of the acceleration, the orbit is changed allowing the electrons to strike a tungsten target, thus producing an X-ray beam in the forward direction of the electrons. A complete description of the mode of operation, and various features of its design and construction has been presented by Elder et al. (1947).

The energy of this X-ray beam is distributed over a spectrum, the maximum being determined by the energy of the electrons. Schiff (1951) has developed a theoretical approach to determine the X-ray spectra from machines operating in this energy range. Spectra obtained from Schiff's expressions are tabulated in Handbook 55 (1954).

The electron energy is continuously adjustable from 5 Mev to 70 Mev. Therefore, the synchrotron is capable of gen-

erating X-ray beams with maximum spectral edges from 5 Mev to 70 Mev. Selected spectral edge points have been calibrated by Anderson and Swift (1970) with an accuracy of about 1%.

General Electric has listed the maximum beam intensity at 300 roentgens per minute at a distance of 1 meter from the target, and the stray radiation to be less than 1 roentgen per hour. Both measurements were evaluated at 70 Mev. More recent measurements have been made with a Victoreen Condenser R-Meter and the maximum beam intensity was found to be 240 roentgens per minute with stray radiation less than 20 milliroentgens per hour.

The beam angle to half maximum intensity is 2° to 3° at 70 Mev. The angle varies approximately as the inverse of Mev. Collimators are available which offer a wide selection of field sizes and shapes.

The duration of the X-ray pulse is in the order of several microseconds. The pulse rate of 60 per second is sufficient for steady state detector operation.

5.2 Phantom Design

Since scattered radiation will contribute to the dose at any point in the medium, the phantom should be sufficiently large to make negligible the effect of increasing its size. To do this, a semi-infinite medium is generally used. This term means that any change in medium shape or volume will not affect absorbed dose measurements at the

point of interest.

Essentially no work has been done on semi-infinite medium design for absorbed dose measurements above 35 Mev. However, backscatter measurements above 35 Mev have indicated that increasing the medium thickness beyond two mean free path lengths does not significantly affect the measurements (Crites, 1970). Since the physical size of the medium is of practical concern, the minimum value of two mean free path lengths was the basis for semi-infinite medium design.

Water is recommended as the medium for absorbed dose measurements (ICRU, 1969) and was used in this study. This material was chosen because its radiation properties are similar to those of most biological tissues and it is a medium in which much information on absorbed dose has been obtained.

The incident photon beam was collimated to twenty-seven centimeters in diameter upon entrance into the medium and the absorbed dose measurements were made at the peak of the depth-dose distribution. At 65 Mev, mean free path length for this energy beam is approximately 50 centimeters. Thus, the phantom design along the central axis of the beam was 110 centimeters. This is the minimum length required for semi-infinite medium design at 65 Mev, considering buildup depth and photon mean free path length.

Scattering material was also needed around the volume of water through which the incident beam passes to insure semi-infinite medium design. Since this material was not within

the primary beam, its thickness was designed on secondary electron range. A 65 Mev X-ray beam generates an electron energy spectrum which has a mean range of approximately 10 cm in water. This case is analogous to the photon case, and two electron range lengths would establish a minimum of 20 centimeters of scattering material outside the primary beam.

From the previous discussion then, the miniumum medium design was established to be 110 centimeters along the central axis of the incident photon beam and 60 centimeters in diameter perpendicular to the central axis. A phantom of these dimensions was constructed of plexiglas for this study. The side and back walls are 9 mm thick, the bottom surface 1 cm thick, and the front or irradiation surface is 6 mm thick.

5.3 Ferrous Sulfate Dosimeters

The ferrous sulfate solution used in this study was prepared by M.D. Anderson Hospital in Houston, Texas. Their standard solution is composed of 0.001 M $FeSO_4$ and 0.001 M NaCl in 0.8 N H_2SO_4. High purity chemicals and water were used in preparing this solution.

Irradiation vessels were constructed of teflon with the following sensitive volume dimensions: 4.6 cm diameter and 0.6 cm depth. The walls of this disk are 0.1 cm thick. The sensitive volume holds 10 ml of solution which allowed for ferric ion determination using a 10 cm absorption cell. Therefore, dose determinations can be made down to several hundred rads with good precision (Shalek and Smith, 1969).

The sensitive volume thickness was determined by the length of the lithium fluoride high sensitivity rods. Both dosimeter types were irradiated with this dimension parallel to the central axis of the primary beam so that absorbed energy would be measured over the same path length. One wall of the vessel is removable for access to the sensitive volume, but forms a water tight seal when in place.

In order to prepare these vessels for dosimetry, they were filled with ferrous sulfate solution and irradiated to 15 megarads to remove any organic impurities originally present in the teflon. The vessels were then filled with fresh ferrous sulfate solution and were ready for use.

After each irradiation, the vessels were returned to M.D. Anderson Hospital for analysis. The ferric ion concentration was measured on a Beckman DU Model 2400 spectrophotometer using a 10 cm absorption cell and a wavelength of 304 nm. The optical density of irradiated solution was obtained along with the optical density of unirradiated solution. From this information, the absorbed dose was calculated by the formula given below (Shalek and Smith, 1969).

$$E_m = \frac{100\ CN}{1{,}000\,[1 + a(t - 25)]\,\epsilon_{304\ nm}\rho_d} \times \frac{D - B}{LG} \times \frac{(\mu_{en}/\rho)_m}{(\mu_{en}/\rho)_d} \text{ rads}$$

The symbols are defined as follows:

E_m = absorbed dose in rads

$C = 1.602 \times 10^{-14}$ rad gm ev^{-1}

$N = 6.023 \times 10^{23}$ molecules mole^{-1}

B = optical density of unirradiated solution

D = optical density of irradiated solution

L = length of the absorption light path in centimeters = 10 cm

$\epsilon_{304\ nm}$ = molar extinction coefficient for ferric ion in liters mole^{-1} cm^{-1} at 304 nm = 2,196 liters mole^{-1} cm^{-1} at 25°C for 0.8 N H_2SO_4

G = molecules of ferric ion formed per 100 ev absorbed

ρ_d = physical density of dosimeter = 1.024 gm cm^{-3} for 0.8 N H_2SO_4

a = fractional increase of extinction coefficient per °C = 0.69% for 0.8 N H_2SO_4

t = temperature of dosimeter in °C at the absorption reading

$(\mu_{en}/\rho)_m$ = mass energy absorption coefficient of medium

$(\mu_{en}/\rho)_d$ = mass energy absorption coefficient of dosimeter

Therefore, for ferrous sulfate solution prepared in 0.8 N H_2SO_4 and read out in a 10 cm absorption cell, the formula above reduces to the following:

$$E_m = \frac{4.291 \times 10^5}{1 + 0.0069\ (t - 25)} \times \frac{D - B}{10G} \times \frac{(\mu_{en}/\rho)_m}{(\mu_{en}/\rho)_d} \text{ rads}$$

This relationship is valid only when electronic equilibrium has been established. This condition can generally be assumed at energies below 0.6 Mev where the measure of absorbed dose is due almost entirely to electrons generated within the dosimeter volume. At higher energies, electrons originating in the buildup material enter the dosimeter volume and contribute to absorbed dose. Corrections for this condition have been discussed in section 4.2 and must be con-

sidered for this calculation.

5.4 Dosimeter Placement

To best compare dose measurements from lithium fluoride and ferrous sulfate dosimeters, the dosimeters should be irradiated under identical conditions. This is best accomplished by simultaneous irradiation to eliminate placement errors and variance in the photon beam.

But for simultaneous irradiation, both dosimeters should be referenced to the same volume within the medium. This is necessary because dose rate not only varies with depth in the phantom, but also across the primary beam.

An irradiation technique has been developed for simultaneous irradiation. Two ferrous sulfate dosimeters were placed equidistant from the center in a circular plexiglas disk. These are shown in Figure 12. The disk was positioned perpendicular to and centered on the incident primary beam. During irradiation the disk was rotated about the central axis. In this way, both dosimeters received the same dose regardless of dose rate or angular distribution of the beam.

The lithium fluoride dosimeters were positioned in the same way. Fifty lithium fluoride dosimeters were arranged in two 5 x 5 matrices as shown in Figure 12. The side dimension of each matrix was the same as the diameter of the ferrous sulfate dosimeter sensitive volume. These matrices were centered at the same distance from the point of rotation as the ferrous sulfate dosimeters.

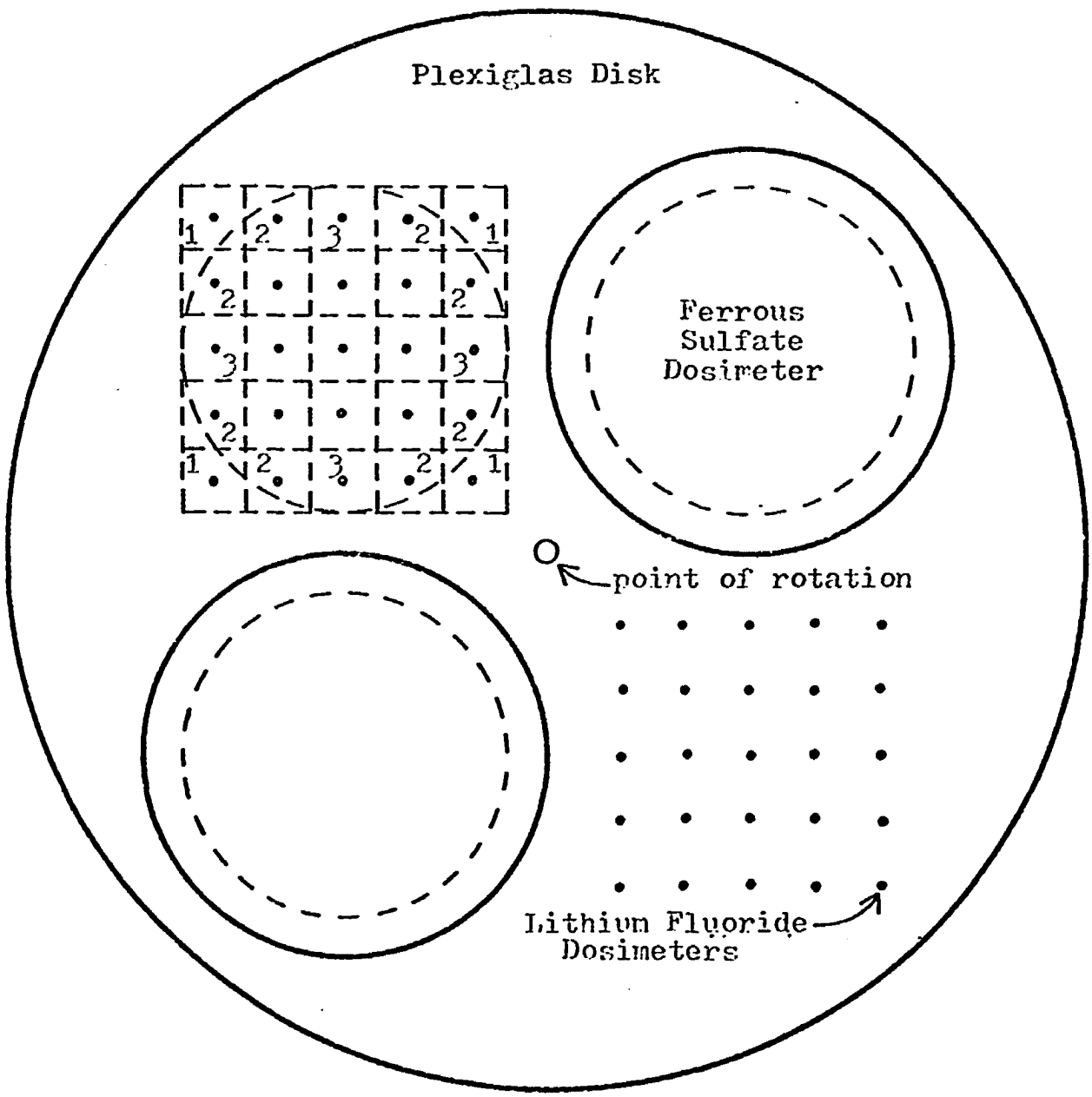

Figure 12. Dosimeter Placement

The matrix in the upper left-hand portion of the plexiglas disk in Figure 12 shows the placement of the lithium fluoride dosimeters. One dosimeter is centered in each square with the 6 mm dimensions parallel to the central axis of the primary beam. The thermoluminescent response of each dosimeter represents the average absorbed dose within its square. Thus, the thermoluminescent response of all 25 dosimeters represents the total absorbed dose within the 5 x 5 matrix.

But the thermoluminescent response within a volume the same shape and size of the ferrous sulfate sensitive volume was needed for comparison. To accomplish this, a circle with dimensions equal to the sensitive volume of the ferrous sulfate dosimeter was inscribed within the matrix. Each dosimeter reading was corrected for the percent of each square lying within the circle. These correction factors were determined using a planimeter and are as follows: squares numbered 1, 13.25%; squares numbered 2, 77.25%; squares numbered 3, 98.25%. All other squares were taken as 100%. The corrected thermoluminescent response represents the total absorbed dose within a volume equal to the sensitive volume of the ferrous sulfate dosimeter.

5.5 Irradiation Technique

Lithium fluoride thermoluminescent dosimetry finds its greatest application in the medical field where it is used to measure therapeutic doses in biological materials. Several hundred rads is representative of therapeutic doses.

It is in this dose range, then, that the thermoluminescent response of lithium fluoride should be established.

The exact dose level to be investigated was established by the sensitivity of the ferrous sulfate dosimeter. It was stated in a previous chapter that with proper precautions, doses can be measured below 400 rads with good precision. This study used the currently acceptable method of ferrous sulfate dosimetry in order to approach this sensitivity. Therefore, 400 rads was selected as the dose level for this study.

It is generally accepted that the dose-response relationship is linear up to about 10^3 rads. Thus, any small variation in dose levels around 400 rads will have no effect on a response per rad relationship.

Photon energies of 35 Mev, 50 Mev, and 65 Mev were selected for this study. The current information on the thermoluminescent response of lithium fluoride covers electron energies to 35 Mev and X-ray energies to 22 Mev. Sixty-five Mev gives a peak dose at about the maximum depth used in therapy. The 35 Mev point was chosen to be a link between the 65 Mev point and existing data. The point at 50 Mev was selected to determine the linearity of the energy-response relationship

Since this study involved a comparison between the energy absorbed in lithium fluoride and the energy absorbed in the medium which the dosimeter material displaces (measured by the ferrous sulfate dosimeter), the depth at which these

measurements were made is not critical. Both lithium fluoride and ferrous sulfate give a measure of absorbed energy, and the ratio of these values is practically constant over the depth-dose distribution.

But for consistency with other published data and considering the depth in matter at which absorbed energy is of interest to the radiotherapist, all measurements of absorbed energy were made at the peak of the depth-dose distribution for the photon energy under consideration. The plexiglas disk containing two ferrous sulfate dosimeters and two sets of lithium fluoride dosimeters were positioned at this depth and rotated slowly while being irradiated. Thus, both dosimetry systems were exposed under identical conditions and can be compared.

Since the measurements were made within water, it was important for the water not to come in contact with the sensitive volume of either dosimetry system. The ferrous sulfate solution was contained within a water tight vessel, so there was no interaction between solution and water. The lithium fluoride dosimeters, however, were placed in holes drilled in the plexiglas disk and measures had to be taken so they would not get wet. The solubility of lithium fluoride is 0.27 grams per 100 ml of water, and water greatly affects thermoluminescent response (Harshaw Chemical Company, 1971). A thin film of plastic was placed over the surface of the plexiglas disk in order to keep water off both the

lithium fluoride and the ferrous sulfate dosimeters during irradiation.

CHAPTER VI

EXPERIMENTAL TESTS AND METHODS

6.1 Effect of Phantom Size on Dose

An investigation was made to determine if the water phantom described in section 5.2 acted as a semi-infinite medium. If this condition was not satisfied, a change in the phantom size would affect dose measurements.

A Victoreen 100R high energy ion chamber was placed at a depth of 10 cm in the water phantom. This position is approximately the peak of the depth-dose distribution for a 65 Mev X-ray beam (Adams and Paluch, 1965).

Exposure was integrated to a reading of 67.6 roentgens on the ion chamber. This measurement was repeated with an additional 30 cm of water placed behind the phantom and again with an additional 30 cm of water placed beside the phantom. The ion chamber readings from these measurements were 67.3 roentgens and 67.5 roentgens respectively. The differences between these readings were less than 1%. Since the precision of ion chamber measurements is considered to be 1 or 2% (Johns, 1961), there was no detectable difference between these three measurements. It was therefore concluded that the phantom was a semi-infinite medium for photon energies up to 65 Mev.

It was not necessary to convert these exposure measurements to absorbed dose in water because the ratio of exposure

measurements are the same as absorbed dose ratios at any given energy level, (Hospital Physicists' Association, 1969).

6.2 Effect of Phantom Material on Dose

An exposure measurement was again made in the water phantom at a depth of 10 cm using a 65 Mev X-ray beam. This was compared with a measurement made under the same conditions but with an additional 9 mm plexiglas sheet added to the inside of the front surface. The ion chamber readings were 33.8 roentgens and 33.7 roentgens respectively. Considering the precision of ion chamber measurements (see section 6.1), these measurements are not significantly different. It was concluded that the 6 mm plexiglas front surface does not significantly affect exposure measurements in water. Measurements made in this phantom are the same as if the entire buildup material consisted of water.

For structural purposes, a front surface of less than 6 mm could not be used. Water pressure caused considerable deviations from flatness when thinner materials were used.

6.3 Depth-Dose Distribution

The Victoreen 100R high energy ion chamber was used to make relative depth-dose measurements at 35 Mev, 50 Mev, and 65 Mev. At each energy, a measurement was made at a depth of 2 cm from the front surface of the phantom. Readings were then made at increasing distances until a maximum dose was reached. This increase in dose is due to the gradual buildup of the electron spectrum in the phantom. Beyond the peak

reading, additional measurements were made at several points through the phantom to establish the exponential fall-off of dose due to attenuation of the primary beam.

The relative depth-dose distributions in water for 35 Mev, 50 Mev, and 65 Mev photon beams are shown in Figure 13. The maximum dose occurs at 6 cm, 7 cm, and 9 cm, respectively. These curves are plotted as a percent of the maximum value.

All measurements were made at the point of maximum dose, which is constant over several centimeters length. Therefore, absorbed dose will be nearly constant through the entire sensitive volume of both the lithium fluoride and ferrous sulfate dosimeters.

6.4 Calibration of Ferrous Sulfate Dosimeters

A group of nine ferrous sulfate vessels were filled with a standard solution by M.D. Anderson Hospital and returned for irradiation. Three were irradiated to 400 rads, four to 1,000 rads, and one to 4,000 rads. One dosimeter was unirradiated and was used as background. The irradiation source was cobalt-60 with a dose rate of 45.7 rads/minute. This was determined by a Victoreen 100R high energy ion chamber along with the appropriate roentgen to rad conversion factor, backscatter factor and percent depth-dose factor from Johns (1961). After irradiation, the nine dosimeters were returned to M.D. Anderson Hospital for dose determination.

The mean values of the readouts at the three dose levels are presented in Figure 14. It can be seen that absorbed

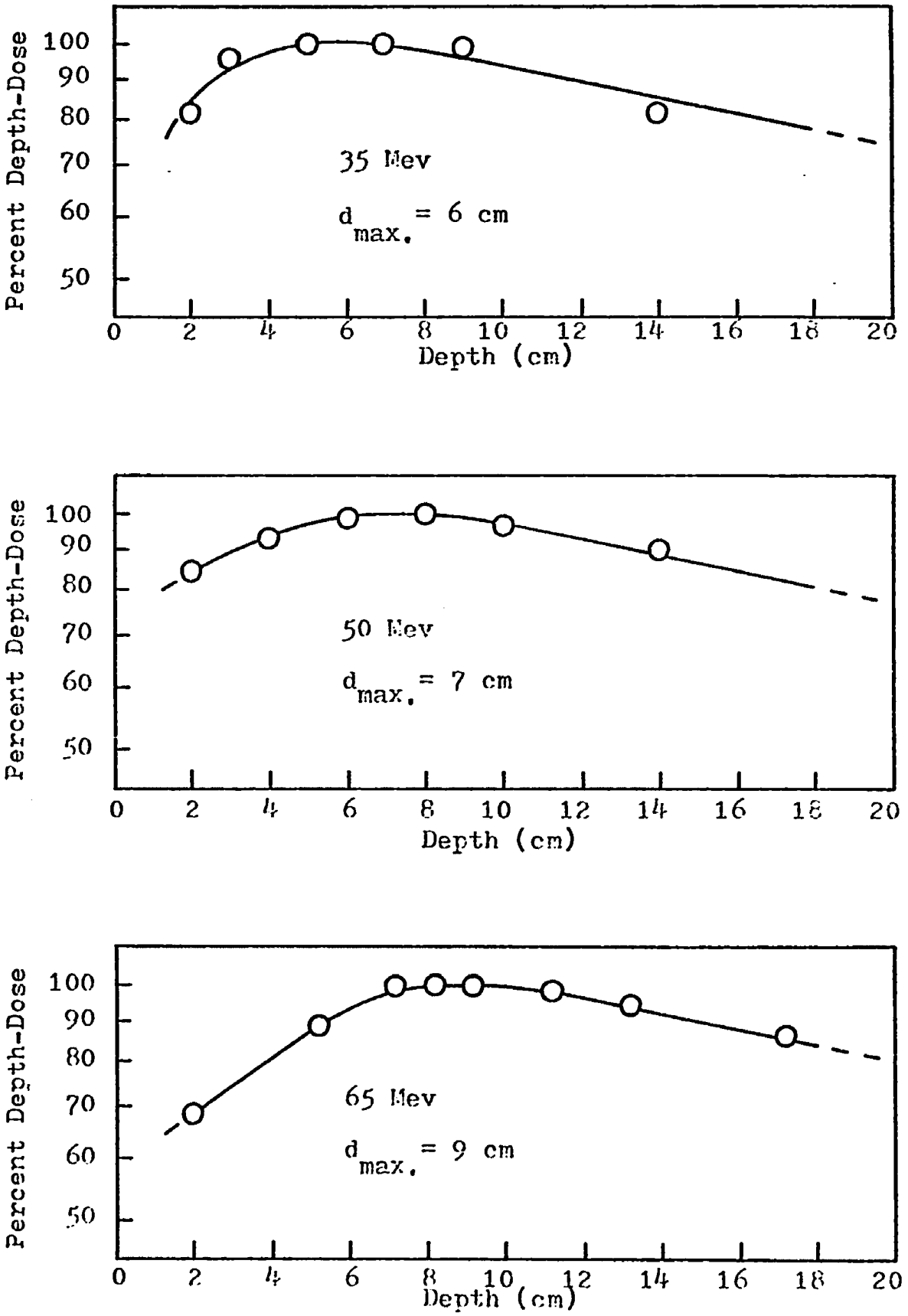

Figure 13. Relative Depth-Dose Distributions for 35 Mev, 50 Mev, and 65 Mev Photon Beams.

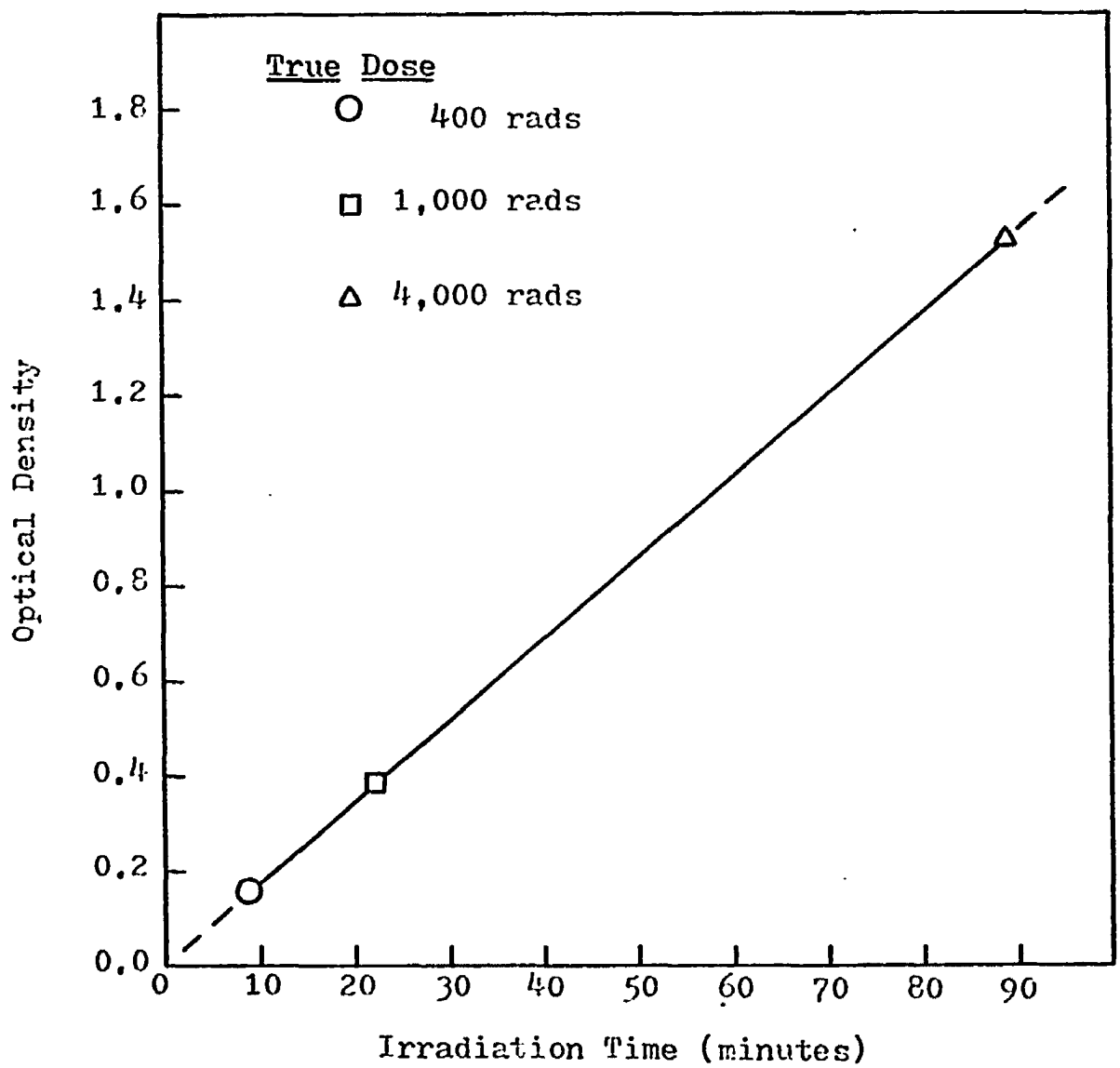

Figure 14. Calibration Curve for Ferrous Sulfate Dosimeters.

dose as measured by ferrous sulfate dosimeters is a linearily increasing function between 400 rads and 1,000 rads. An extrapolation of this curve passes through the origin which indicates that impurities are not present in amounts sufficient to affect ferric ion concentration.

Since optical density is proportional to absorbed dose, the slope of the curve represents the dose rate as measured by these dosimeters. The dose rate was calculated from the expression in section 5.3 by using the slope in place of (D - B) in the equation. This calculation showed a dose rate of 45.9 rads/minute. There is less than 0.5% difference between this value and the true dose rate. This difference is well within the overall experimental error of this study; therefore, ferrous sulfate dosimetry was used to give a measure of the true absorbed dose in the phantom at the 400 rad dose range. The standard deviation associated with the point at 400 rads is 4% of the mean. This could not be shown in Figure 14 due to the large scale.

Nine ferrous sulfate dosimeters were again prepared by M.D. Anderson Hospital and returned for use. They were held for two weeks and then mailed back to M.D. Anderson for dose determination. This was done to establish the background levels associated with mailed dosimeters. The mean response of these dosimeters was equivalent to a dose of less than 10 rads when compared to the response of freshly prepared ferrous sulfate solution. This value is small when compared to an

irradiation dose of 400 rads. An unirradiated dosimeter was read out with each group of irradiated dosimeters to account for the background dose.

6.5 Calibration of Lithium Fluoride TLD-700 Dosimeters

Thermoluminescent dosimetry is not a system of absolute dosimetry since it measures only relative response. Meaningful interpretation can only be made through a comparison of thermoluminescent response to a known dose. The best way to calibrate this dosimetry system is to expose the dosimeters to a dose which has been determined by an absolute technique. In this way, a calibration factor can be obtained to accurately convert thermoluminescent response to absorbed dose.

The accuracy of a particular dose measurement is defined as the difference between the measured dose and the true dose. The two most important components of this difference are associated with the calibration factor and the non-linearity of dosimeter response to parameters like energy, dose-rate, and total dose. Since all parameters except energy were accounted for during this study, the difference between measured dose and true dose can be attributed to energy dependence.

The precision of the thermoluminescent dosimetry system refers to the variation in thermoluminescent response among dosimeters exposed to the same dose. This is expressed as the standard deviation in such a series of measurements. Two components of this variation are sensitivity variation, which is proportional to dose, and background variation, which is

independent of dose.

Background variation determines the minimum dose that can be measured and is generally constant. This variation is of consequence only when small doses are measured. Sensitivity variation, however, is affected by parameters like size of dosimeter, optical density of the dosimeter, and thermal annealing effects. The parameters for a given batch of dosimeters are fixed and precision can be determined by measuring the thermoluminescent response of each dosimeter exposed to the same dose. Thermal annealing effects can be controlled as explained later in this section.

Initially a batch of 100 lithium fluoride TLD-700 high sensitivity rods was selected for this study. The entire batch was irradiated to 400 rads of cobalt-60 gamma rays. The standard deviation of the readouts was 11% of the mean. From this batch, the 75 dosimeters whose response was closest to the mean were selected. Recalculation of the statistics for this group showed a standard deviation of 3.6% of the mean. This is within the range of 4% quoted by Harshaw Chemical Company.

Since thermoluminescent response is directly proportional to dosimeter size, it was decided to compare the statistics on dosimeter weight with the statistics on response given above. Each dosimeter in the initial batch of 100 was weighed. The mean weight was 15.5 mg and the standard deviation of these weights was 11% of the mean. Recalculations of the

statistics for the group of 75 dosimeters selected above showed a mean of 16.0 mg and a standard deviation of 2.7% of the mean. Therefore, there is close agreement between dosimeter size and thermoluminescent response. The group of 75 dosimeters selected above were used in this study.

The relative magnitude of the glow curve peaks after irradiation is highly dependent on pre-irradiation heat treatment. The pre-irradiation annealing procedure adopted for this study was that proposed by Cameron et al., (1964). Their standard procedure begins by annealing the dosimeters for one hour at 400°C±25°C in a pre-heated oven. This empties all traps in the phosphor. The dosimeters are then cooled to 80°C in 10 to 20 minutes (Zimmerman et al., 1966). After cooling, the dosimeters are annealed for 24 hours at 80°C±2°C in a pre-heated oven. This anneal arranges the distribution of traps within the crystal so the main dosimeter peak at 190°C predominates, and makes the contribution from the low temperature peaks as small as possible. At the end of this anneal they are cooled to room temperature and are ready for use.

With this procedure, the low temperature peaks contribute only a few percent to the total thermoluminescence. Even this can be reduced by waiting at least 10 minutes after irradiation for readout to allow these effects to decay out. Additionally, a 140°C pre-heat anneal was used during the readout cycle to further reduce these effects (Eberline Instrument Company, 1969).

This standard procedure was used before each irradiation. It was followed as closely as possible so the dosimeter trapping characteristics would be the same for each irradiation. This procedure will restore the trapping characteristics to as near as possible to those originally present.

But even with this annealing procedure it can not be assumed that the calibration factor will be the same for every irradiation. In fact, sensitivity within the same batch of dosimeters has varied as much as 35% between irradiations (Beck et al., 1968). The response of each dosimeter with respect to the mean response of the batch changed by approximately the same percent between irradiations.

To determine a calibration factor for each irradiation, the following technique was used.

1. Anneal all 75 dosimeters by the standard procedure.

2. Take a random sample of 25 dosimeters from the batch and irradiate to a known dose of about 400 rads. Read these dosimeters and determine a mean thermoluminescent response per rad calibration factor.

3. Use the calibration factor in step 2 to normalize the readouts of the remaining 50 dosimeters used in this study.

In order to establish a background for undosed lithium fluoride, 25 dosimeters were irradiated to about 400 rads by cobalt-60 gamma rays. They were then annealed by the standard procedure and read out. The mean of the readings was equivalent to 200 mrads. This procedure was repeated

but with 0.5 liters per minute of nitrogen gas flowing through the heater pan. The mean of the readings was reduced to less than 100 mrads. This was considered to be insignificant when compared to the dose level of 400 rads used in this study.

The background using nitrogen gas was again determined at the end of this study and it did not differ from the results above. For this reason, it was not necessary to make background corrections. Nitrogen gas was used during the entire study to minimize background.

To investigate the effect of total dose on thermoluminescent response, the 75 dosimeters were divided into 15 groups of 5 dosimeters each. Each group was irradiated to a different dose level between 100 rads and 1,000 rads. A plot of the mean response of each group is shown in Figure 15. The standard deviation of each mean could not be plotted due to the large scale. The average standard deviation, however, was 2.2% of the mean; the smallest being 0.7% at 500 rads and the largest being 3.4% at 750 rads.

The relationship between thermoluminescent response and absorbed dose is linear up to 550 rads. The line of linearity is within one standard deviation of every mean in the dose range between 100 rads and 550 rads. Above 550 rads, thermoluminescent response increases faster than proportionally to absorbed dose, that is it becomes supralinear. During the course of this study no measurements were made in the supralinear region.

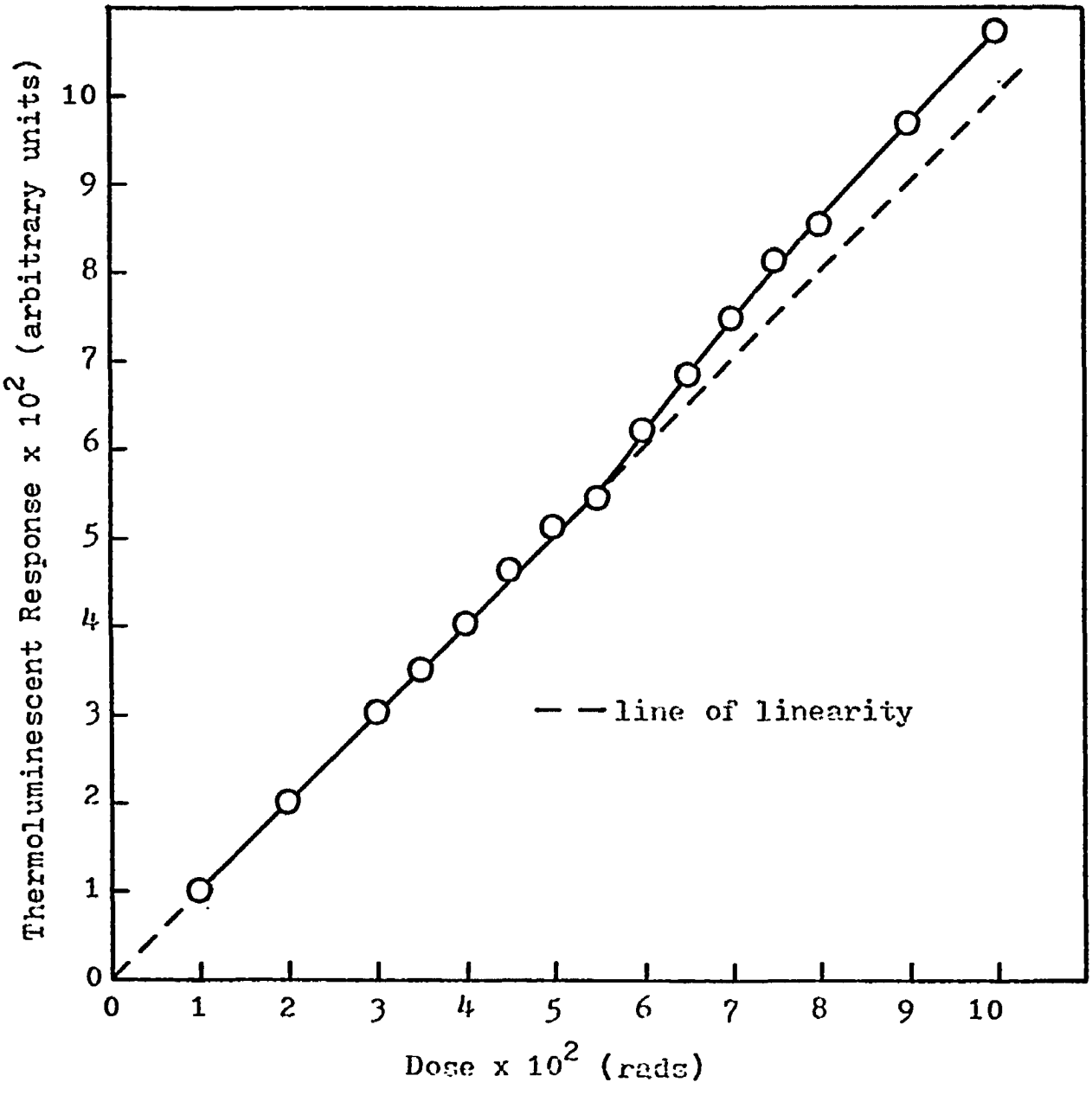

Figure 15. Dose-Response Curve of Lithium Fluoride TLD-700.

6.6 Response of Lithium Fluoride to Mixed Radiation Field

An approximate determination of the neutron and photon components in a mixed radiation field can be made by irradiating TLD-100 in combination with TLD-700. The TLD-700 gives essentially the photon component which can be used to correct the reading of the other phosphor to obtain thermal neutron response.

Any attempt to determine the neutron contribution to the total response of TLD-700 in a mixed field becomes a complex problem. Two major complications arise: one, the glow curve produced by neutrons is slightly different from that produced by photons; and two, TLD-100 and TLD-700 respond differently to photon irradiation.

Reddy et al. (1969) have developed a technique for measuring both neutron and photon components in a mixed field. They determined the ratio between neutron and photon glow curve peak heights. From this analysis, it was determined that the thermoluminescent response of TLD-700 to 400 rads of cobalt-60 gamma rays was equivalent to a thermal neutron flux of about 5×10^{11} n/cm^2. Equivalent photon-neutron doses were not determined for neutron flux below 10^{11} n/cm^2. So, from this information, a neutron flux considered to be insignificant compared to a 400 rad photon dose could not be determined.

Mason (1970) has established that the ratio of thermal neutron flux rate to photon dose rate is the critical factor

in determining whether or not the neutron component contributes significantly to the thermoluminescent response of Type 7 lithium fluoride. His calculations show that Type 7 is insensitive to thermal neutrons in a mixed field for which $\phi/R < 10^4$, where ϕ is the thermal neutron flux rate (n/cm^2 sec) and R is the photon dose rate (mrad/sec).

The maximum dose rate obtained under the conditions of this study was approximately 10 rads/minute. This was the average dose rate across the dosimeter volumes. The central axis dose rate was approximately ten times this value.

Using the ϕ/R ratio of Mason, Type 7 lithium fluoride will be insensitive to a thermal neutron flux rate of less than $10^6 n/cm^2 sec$ in a mixed field containing a photon dose rate of 10 rads/minute. The maximum thermal neutron flux rate resulting from the photoneutron reaction is in the range 10^2 to $10^4 n/cm^2 sec$ (Adams and Paluch, 1965). This was measured along the central axis of a 70 Mev X-ray beam. A smaller flux rate would be expected at the dosimeter location. Therefore, the thermal neutron flux rate at the dosimeter location is several orders of magnitude less than the minimum detectable value of $10^6 n/cm^2 sec$ obtained from Mason's work.

Since lithium fluoride Type 7 is isotopically similar to lithium fluoride TLD-700, a similar response would be expected from the TLD-700 material. Therefore, the thermoluminescent response of lithium fluoride TLD-700 in this

study was a measure of only the photon component in the mixed field.

In order to justify this conclusion, 25 TLD-700 dosimeters and 25 TLD-100 dosimeters were irradiated simultaneously to approximately 400 rads by a 65 Mev photon beam. This energy was selected since photoneutron yield increases with increasing energy. The mean of each group was calculated and the ratio of TLD-700 response to TLD-100 response was 0.81. This procedure was repeated with cobalt-60 gamma irradiation and the ratio of TLD-700 response to TLD-100 response was again 0.81.

Since TLD-100 contains 7.5% lithium-6 and TLD-700 contains only 0.007% lithium-6, a smaller TLD-700 response to TLD-100 response ratio would be expected if there was a significant neutron component in the mixed field. Since this was not the case, both TLD-100 and TLD-700 lithium fluoride response was due solely to the photon component.

No attempt was made to measure the thermoluminescent response to the fast neutron component in the mixed field. The following argument is justification for neglecting this component.

An approximation for the neutron energy distribution in water assumes the high energy tail has an E^{-1} energy dependence (Adams and Paluch, 1965). Therefore, the fast neutron flux rate should be less than the maximum thermal neutron flux rate of $10^4 n/cm^2 sec$. For an average run time of 40

minutes to accumulate 400 rads operating at 65 Mev, the thermal neutron flux would be less than $10^8 n/cm^2$. Assuming the fast neutron flux is less than the thermal neutron flux, the dose contribution from fast neutrons is less than 1 rad in a mixed field whose photon component is 400 rads. This is based on the thermoluminescence from either TLD-100 or TLD-700 exposed to 10^8 fast neutrons/cm^2 being less than when exposed to one roentgen of photon irradiation (see section 3.7). One rad is considered insignificant when compared to the photon component of 400 rads.

6.7 Experimental Technique

The centerline of the water phantom was positioned on beam center with a target to front surface distance of 150 cm. Alignment was obtained visually by placing cross hairs in the center of the beam port and at beam center on the primary barrier.

The primary beam was measured by photographic film to be 27 cm in diameter at the front surface of the phantom. The film also confirmed that the phantom was properly aligned on the beam.

The plexiglas disk which held the 2 ferrous sulfate dosimeters and 50 lithium fluoride dosimeters was mounted on a plexiglas shaft and suspended from the top of the phantom by 2 plexiglas arm brackets. These hold the shaft on the centerline of the incident photon beam and allow the disk to rotate freely about the centerline. This entire

assembly could be positioned at any point along the length of the phantom allowing the disk to be positioned at any depth from the front surface. Rotation was powered by a DC motor mounted on top of the arm bracket mount. The motor shaft was connected to the disk by means of an O-ring. Rotation speed was set at 1 revolution every 4 seconds. This setup is shown in Figure 16.

A plexiglas cylinder extending from the top of the phantom down through the centerline of the incident photon beam was used to hold a 100R high energy Victoreen ion chamber with its sensitive volume centered in the beam. A plug was put in the bottom end to make the cylinder water tight. It was positioned in the rear of the phantom, 100 cm from the front surface. The ion chamber could be removed from the cylinder for readout. This chamber was used to measure integrated exposure and is shown in Figure 16.

The relationship between ion chamber exposure and the average absorbed dose to the ferrous sulfate dosimeters was established at 35 Mev, 50 Mev, and 65 Mev. With a monitor on the integrated exposure, dose levels of approximately 400 rads to the ferrous sulfate dosimeters were easy to obtain.

Fifty lithium fluoride TLD-700 dosimeters were selected at random from the batch of 75 and placed in the plexiglas disk. Each matrix contained 25 dosimeters. A layer of thin plastic tape was placed over the disk surface to prevent

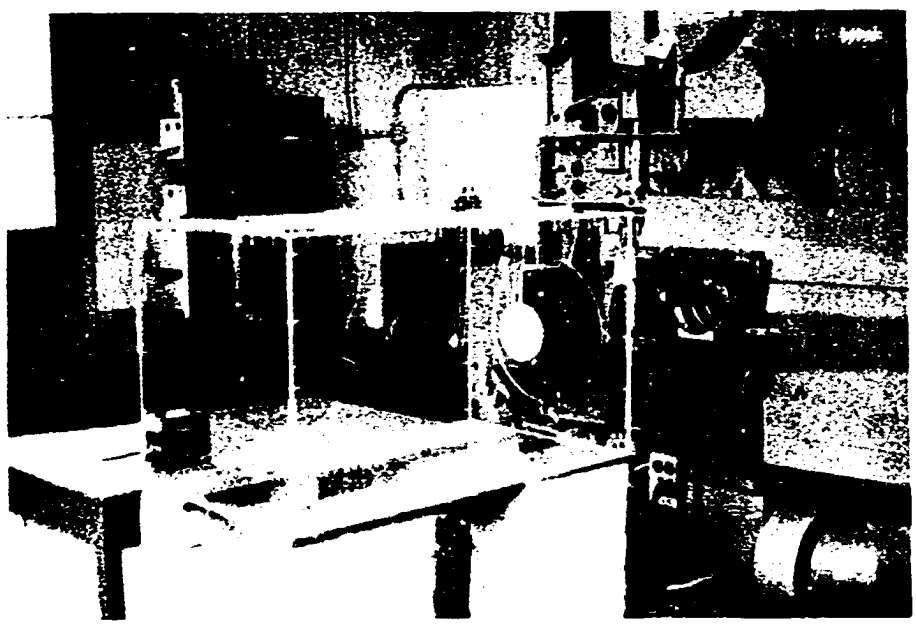

Figure 16. Experimental Setup Showing Synchrotron Irradiation Port, Water Phantom, and Dosimeter Mount.

water from reaching the dosimeters. Two ferrous sulfate dosimeters were placed in the disk and taped into place. The disk was then mounted into the arm brackets and the entire assembly placed in the water phantom. The distance from the front surface of the phantom to the center of the disk was adjusted to the depth of maximum dose for the energy under consideration. The ion chamber was charged and placed in the rear of the phantom. The setup was then ready to be irradiated at the energy under consideration.

After irradiation, all dosimeters were removed from the disk and prepared for readout. The two ferrous sulfate dosimeters along with a blank were sent to M.D. Anderson Hospital for readout. Once the ferric ion concentration and temperature of readout had been determined, absorbed dose in water was calculated by the method outlined in section 5.3.

Readout of the first matrix of 25 dosimeters was done in the order as shown in Figure 17. It was necessary to keep track of the position of each dosimeter so the appropriate square to circle correction factor could be applied (see section 5.4). Each dosimeter reading was multiplied by the appropriate square to circle correction factor to obtain the portion of thermoluminescent response lying inside a volume equal to the sensitive volume of the ferrous sulfate dosimeter.

The individual corrected values were summed over the matrix and divided by 19.64, which is the area of the circle

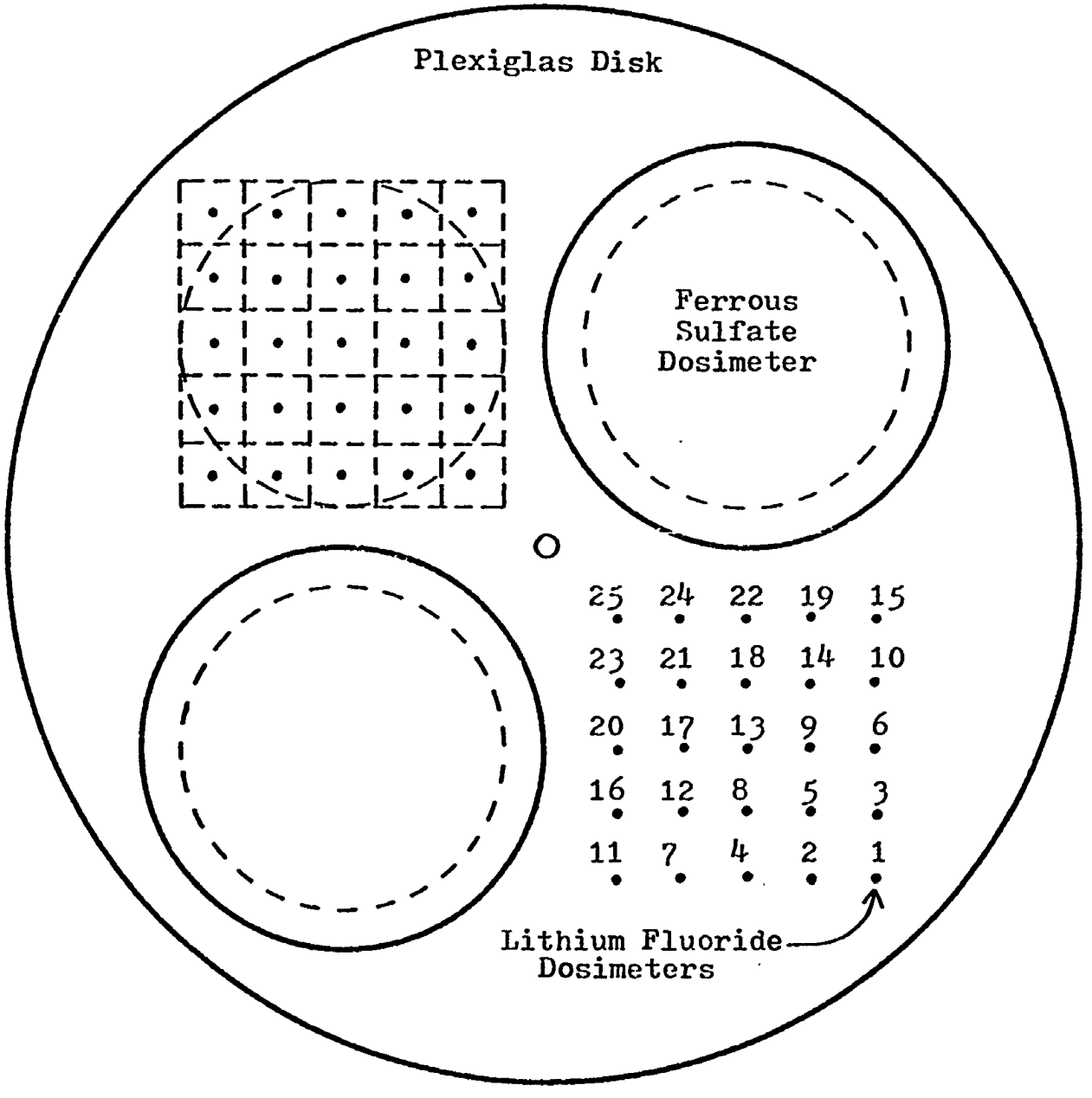

Figure 17. Order of Lithium Fluoride Dosimeter Readout.

inscribed inside the 25 square unit matrix. This gives an average thermoluminescent response per dosimeter within a volume corresponding to that of the ferrous sulfate dosimeter sensitive volume. This readout procedure was repeated on the other matrix and the two values averaged.

The doses calculated from both ferrous sulfate readouts were averaged. This value was used to normalize the average thermoluminescent response to obtain a response per rad for the energy under consideration.

In order to establish a calibration factor, the remaining 25 lithium fluoride TLD-700 dosimeters were irradiated to 400 rads by cobalt-60 gamma rays. Calibration of the cobalt-60 source, in terms of rads in water, was done by means of a 100R high energy Victoreen ion chamber with a National Bureau of Standards derived cobalt-60 gamma ray correction factor, and by applying the appropriate roentgen to rad conversion factor, backscatter factor, and percent depth-dose factor from Johns (1961).

The total thermoluminescent response of all dosimeters was divided by 25 to give the average response per dosimeter. Normalizing this value to 400 rads in water establishes the calibration factor (response per rad) for the other 50 dosimeters irradiated by high energy photons.

The response per rad to high energy photons was then divided by the response per rad to cobalt-60 gamma rays. This gives a response relative to cobalt-60 and allows for

the detection of a difference in response between cobalt-60 and high energy photons.

This entire procedure was run 5 times at each of the following energies: 35 Mev, 50 Mev, and 65 Mev. Between each run, the standard annealing cycle was used. A sample calculation for one run at one energy is shown in Appendix A.

CHAPTER VII

RESULTS AND CONCLUSIONS

7.1 Measured Thermoluminescent Response

The measured values of the thermoluminescent response per rad normalized to cobalt-60 gamma rays are shown in Table 2. Each value represents an average for one run; that is, an average thermoluminescent response of the two matrices of 25 TLD-700 dosimeters each divided by the average absorbed dose of the two ferrous sulfate dosimeters and normalized by the thermoluminescent response per rad for cobalt-60 gamma rays.

The mean value $\bar{X}$ was calculated by summing the individual values X_i and dividing by the number of values, n, i.e.

$$\bar{X} = \frac{\sum X_i}{n}$$

The standard deviation of the mean was calculated from the expression

$$S_{\bar{X}} = \frac{S}{\sqrt{n}}$$

where S is the standard deviation of the individual values, i.e.

$$S = \sqrt{\frac{\sum X_i^2 - n\bar{X}^2}{n - 1}}$$

The mean and standard deviation have been plotted in Figure 18 along with the corresponding calculated values from the next section for cobalt-60 gamma rays and 35 Mev,

Table 2. Measured Thermoluminescent Response of Lithium Fluoride TLD-700 High Sensitivity Rods to High Energy Photons Relative to Cobalt-60 Gamma Rays.

Energy (Mev)	Thermoluminescent Response per Rad (normalized to cobalt-60)	Mean $(\bar{X})$	Standard Deviation of Mean $(S_{\bar{x}})$
35	0.918 0.912 0.882 0.891 0.893	0.899	0.007
50	0.880 0.908 0.930 0.896 0.922	0.907	0.009
65	0.898 0.944 0.893 0.919 0.879	0.907	0.011

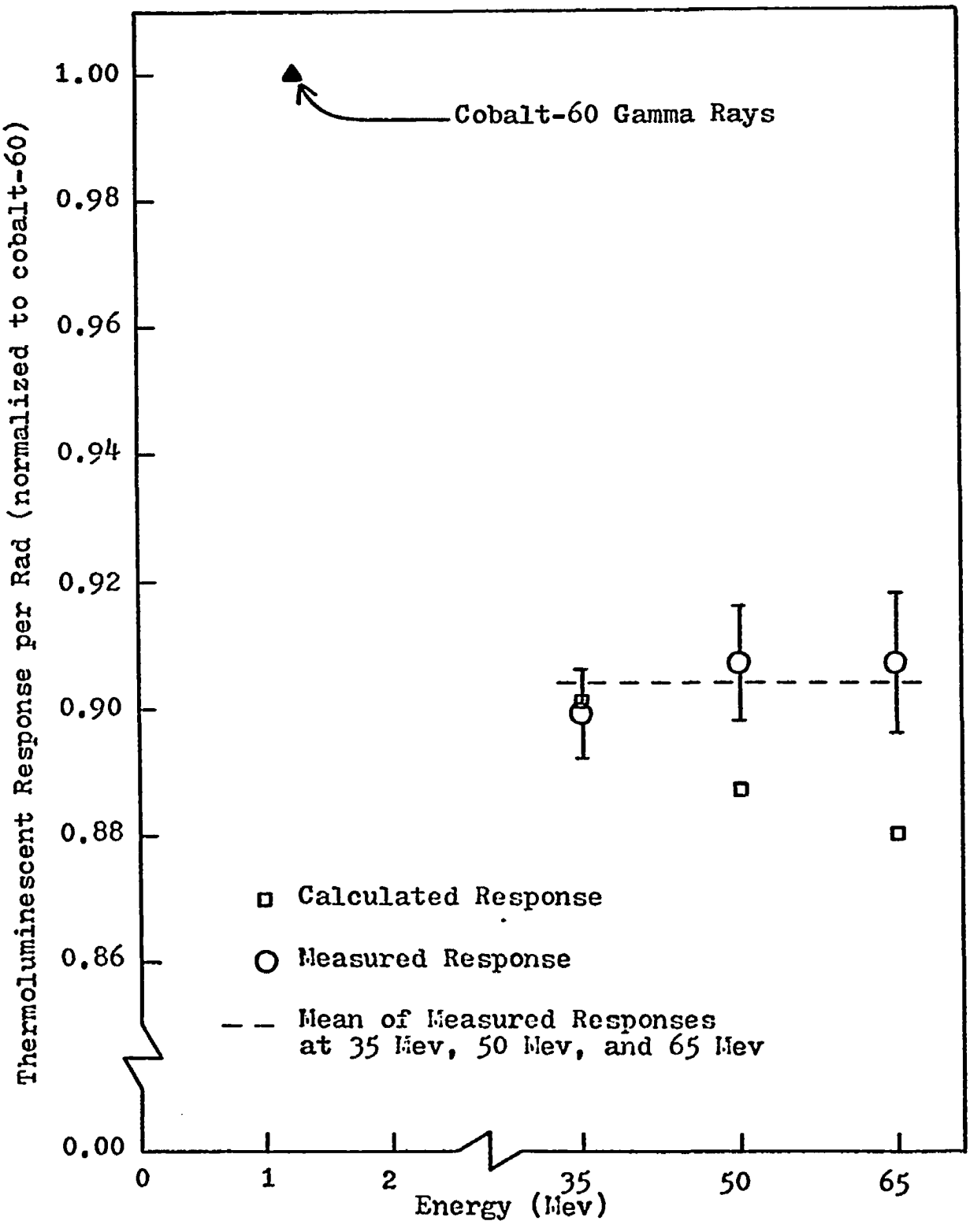

Figure 18. Calculated and Measured Thermoluminescent Response of Lithium Fluoride TLD-700 to High Energy Photons Relative to Cobalt-60 Gamma Rays.

50 Mev, and 65 Mev photons. The dotted line represents the mean of the measured responses at the three high energy photon levels.

7.2 Calculated Thermoluminescent Response

The expected thermoluminescent response was calculated using the general cavity theory derived by Burlin (1966; 1968; Burlin and Chan, 1967) and extended to include high energy electrons and X-rays by Almond and McCray (1970). This theory was developed in section 4.2.

The ratio of absorbed dose in the lithium fluoride dosimeter to the absorbed dose in the water medium is given by the relationship:

$$f = \frac{D_{LiF}}{D_{H_2O}}$$

The thermoluminescent response to high energy photons relative to the thermoluminescent response to cobalt-60 gamma rays is given by f_r in the following expression:

$$f_r = \frac{f_{Photons}}{f_{Co\text{-}60}} = \frac{(D_{LiF}/D_{H_2O})_{Photons}}{(D_{LiF}/D_{H_2O})_{Co\text{-}60}}$$

From the theory developed in section 4.2, the f for both high energy photons and cobalt-60 is calculated from the following expression:

$$f = d \frac{1}{S_{LiF}^{H_2O}} + (1 - d) \frac{(\mu_{en}/\rho)_{LiF}}{(\mu_{en}/\rho)_{H_2O}}$$

Some general assumptions were made in calculating d. The mean free path across the dosimeter, g, was taken as 6 mm. This length was positioned parallel to the incident radiation. Using this value for g assumes that only the primary radiation contributes to absorbed dose. There is, however, a small contribution from secondary radiation. This value is an over estimate for the mean free path across the dosimeter which, in effect, under estimates d. But, d will only increase by about 1% using a g value of 5 mm, so the original value of 6 mm was used. Also, the expression to calculate β was for beta rays in aluminum. This expression was used because the density of lithium fluoride is close to the density of aluminum, and no emperical expression was available for lithium fluoride. β, however, is not greatly affected by density so the expression for aluminum should be good to a first approximation for lithium fluoride. In spite of these assumptions, the calculated values of d do show an increase with increasing energy. This was the expected response.

The mass energy absorption coefficients were taken from Hubbell (1969) and from Evans (1968). They were evaluated from the coefficients μ_{en}/ρ_i for the constituent elements and weighted proportionally according to the weight of the $i^{\underline{th}}$ constituent. The mass stopping powers were obtained from Berger and Seltzer (1964).

Both the mass energy absorption coefficients and mass

stopping powers were determined at the mean secondary electron energy, which was assumed to be one-third of the maximum photon energy (Johns, 1961)... The exact mean electron energy is not critical since the ratio of absorption coefficients and the ratio of stopping powers are used in calculating f. These ratios are fairly constant over the entire energy range under consideration.

The calculated values for f_r are shown in Table 3. These values have also been plotted in Figure 18 to show the comparison between calculated and measured response.

7.3 Conclusions

The results of the experimental measurements normalized to cobalt-60 gamma rays show a 10% decrease in thermoluminescent response from cobalt-60 gamma rays to high energy photons. There was, however, no difference among the responses at the three high energy photon levels to within approximately 1%. The mean of the responses at 35 Mev, 50 Mev, and 65 Mev falls well within one standard deviation of each individual value.

Cavity theory predicts the 10% decrease in thermoluminescent response from cobalt-60 gamma rays to high energy photons. But the theoretical approach also predicts a 2% decrease in sensitivity from 35 Mev to 65 Mev. The calculated value at 35 Mev falls within one standard deviation of the measured value; but at 65 Mev, the calculated value is approximately two standard deviations below the measured value.

Table 3. Calculated Thermoluminescent Response of Lithium Fluoride TLD-700 High Sensitivity Rods to High Energy Photons Relative to Cobalt-60 Gamma Rays.

Radiation	Thermoluminescent Response per Rad (normalized to cobalt-60)
35 Mev Photons	0.901
50 Mev Photons	0.887
65 Mev Photons	0.880

A possible explanation for the decrease in calculated values with increasing photon energy lies in the dosimeter configuration. If the dosimeter dimension is small compared with the electron ranges, the value of d approaches 1 for both cobalt-60 gamma rays and high energy photons. Since the mass stopping power ratio of lithium fluoride to water is relatively constant through this energy range, no decrease in response with energy would be found.

This was verified by cavity theory calculations for a 1 mm thick dosimeter. The calculated sensitivities relative to cobalt-60 gamma rays for 35 Mev and 65 Mev X-ray beams were 0.891 and 0.889 respectively. Thus, a 1 mm thick dosimeter will show approximately a 10% decrease in sensitivity from cobalt-60 gamma rays to 35 Mev X-rays but no further decrease up to 65 Mev.

Since the measured responses from 35 Mev to 65 Mev act as though the dosimeter dimension is small compared with the electron ranges, the assumed value of g (6 mm) in calculating d could have been an overestimate. By assuming a smaller value of g, a 10% decrease in sensitivity from cobalt-60 gamma rays to 35 Mev X-rays could be predicted with no further decrease with increasing energy up to 65 Mev. But no expression was available to give a better estimate of g. Thus, the physical dimension of the dosimeter was used in the theoretical calculation.

Agreement between measured and calculated values is good

considering the assumptions made in the theoretical approach. But if cavity theory is to be used to predict thermoluminescent response to high energy radiations with precision of less than a few percent, additional work needs to be done in refining the assumptions made in the theoretical approach.

CHAPTER VIII

SUMMARY

Most recent investigators have found a ten percent decrease in thermoluminescent response per rad for lithium fluoride from cobalt-60 gamma rays to electrons and X-rays up to 35 Mev. This decrease was predicted from cavity theory calculations. This study confirmed the ten percent decrease in response using lithium fluoride TLD-700 high sensitivity rods in the 35 Mev to 65 Mev X-ray energy range.

A few of the investigators observed a decrease in response with increasing electron or X-ray energy, and this decrease was faster than predicted from cavity theory calculations. In this study, however, no difference was observed between the measured thermoluminescent responses at 35 Mev, 50 Mev, or 65 Mev. Cavity theory predicted approximately a one percent decrease in response over this energy range, but considering the approximations used in this calculation, the predicted response can be assumed to be flat.

In radiation dosimetry, thermoluminescent dosimeters are usually calibrated with cobalt-60 in order to make dose determinations at different energies. This study has extended the usefulness of this procedure to 65 Mev.

APPENDIX A

SAMPLE CALCULATION OF THE THERMOLUMINESCENT RESPONSE PER RAD FOR HIGH ENERGY PHOTONS RELATIVE TO COBALT-60 GAMMA RAYS

Table 5 gives an example of the method used to determine the thermoluminescent response per rad for high energy photons relative to cobalt-60 gamma rays. The third run at 65 Mev will be used to illustrate this calculation.

Table 4. Worksheet for Calculating the Thermoluminescent Response per Rad Relative to Cobalt-60 Gamma Rays for the Third Run at 65 Mev.

65 Mev Photons

Position	Thermoluminescent Response		Square to Circle Correction Factor	Corrected Thermoluminescent Response	
	Matrix 1	Matrix 2		Matrix 1	Matrix 2
1	2752	2719	0.1325	365	360
2	2627	2516	0.7725	2029	1944
3	2956	2929	0.7725	2284	2263
4	2894	2944	0.9825	2843	2892
5	2936	3090	1.0000	2936	3090
6	3111	3009	0.9825	3057	2956
7	3431	3331	0.7725	2650	2573
8	3391	3500	1.0000	3391	3500
9	3084	3546	1.0000	3084	3546
10	3469	2817	0.7725	2680	2176
11	3348	3637	0.1325	444	482
12	3742	3433	1.0000	3742	3433
13	4143	3624	1.0000	4143	3624
14	3453	3572	1.0000	3453	3572
15	3478	3312	0.1325	461	439
16	3654	4166	0.7725	2823	3218
17	4063	4065	1.0000	4063	4065
18	4203	3861	1.0000	4203	3861
19	3883	3785	0.7725	3000	2924
20	5045	4577	0.9825	4957	4497
21	4353	4829	1.0000	4353	4829
22	4381	4497	0.9825	4304	4418
23	5134	5131	0.7725	3966	3964
24	4980	4910	0.7725	3847	3793
25	5711	6421	0.1325	757	851
		Totals	19.64	73835	73270

$$\text{Matrix 1 TL Response per Dosimeter} = \frac{73835}{19.64} = 3759$$

$$\text{Matrix 2 TL Response per Dosimeter} = \frac{73270}{19.64} = 3731$$

Average TL Response per Dosimeter = 3745

Table 4. (continued)

Ferrous Sulfate Dosimeter 1 = 410 rads

Ferrous Sulfate Dosimeter 2 = 426 rads

Average Rads in Water = 418

$$\text{TL Response per Rad} = \frac{3745}{418} = 8.959$$

Cobalt-60 Gamma Rays

Thermoluminescent Response of 25 Dosimeters

4116	4173	4100	3800	4204
4382	4092	3516	3928	4045
3743	3742	4554	3862	4007
3635	3868	4166	3755	4509
4084	4264	4104	3717	3925

Total TL Response = 100291

$$\text{Average TL Response per Dosimeter} = \frac{100291}{25} = 4012 \pm 263$$

Rads in Water = 400

$$\text{TL Response per Rad} = \frac{4012}{400} = 10.030$$

$$\frac{(\text{TL Response per Rad})_{65\ \text{Kev}}}{(\text{TL Response per Rad})_{\text{Co-60}}} = \frac{8.959}{10.030} = 0.893$$

BIBLIOGRAPHY

Adams, G.D., and Paluch, I.R., 1965. "Neutron Measurements Relating to Patients Treated with X-rays from 70 Mev Sychrotron." Physics in Medicine and Biology, vol. 10, pp. 335-344.

Aitken, M.J., Reid, J., Tite, M.S., and Flemming, S.J., 1967. "Quenching of Spurious Thermoluminescence by Nitrogen." Luminescence Dosimetry, pp. 490-501. Proc. Int. Conf., Stanford, 1965. AEC Symp. Ser., vol. 8. CONF-650637. USAEC.

Almond, P.R., 1966. "The Physical Measurements of Electron Beams from 6-18 Mev." Physics in Medicine and Biology, vol. 11, p. 146 (abstract).

Almond, P.R., 1968. "C_λ Values for High Energy X-radiation." Physics in Medicine and Biology, vol. 13, pp. 285-286.

Almond, P.R., and McCray, K., 1970. "The Energy Response of LiF, CaF_2, and $Li_2B_4O_7$:Mn to High Energy Radiations." Physics in Medicine and Biology, vol. 15, pp. 335-342.

Almond, P.R., Wright, A., and Lontz, J.F., 1967. "The Use of Lithium Fluoride Thermoluminescent Dosimeters to Measure the Dose Distribution of a 15 Mev Electron Beam." Physics in Medicine and Biology, vol. 12, pp. 389-394.

Anderson, D.W., and Swift, S.C., 1970. "Energy Calibration Points for Clinical Electron Accelerators." Physics in Medicine and Biology, vol. 15, pp. 349-354.

Beck, W.L., Callis, B.L., and Cloutier, R.J., 1968. "Phantom Depth-Dose Measurements with Extruded LiF in a Low-Exposure-Rate Total-Body Irradiator." Proceedings of the Second International Conference on Luminescence Dosimetry, pp. 976-969. Gatlinburg, 1968. CONF-680920. USAEC.

Benner, S., Johansson, J.M., Lindskoug, B., and Nyman, P.T. 1967. "A Miniature LiF Dosimeter for In Vivo Measurements." Solid State and Chemical Radiation Dosimetry in Medicine and Biology, pp. 65-73. Symp. Proc., Vienna, 1966. STI/PUB/138. IAEA.

Berger, M.J., and Seltzer, S.M., 1964. "Tables of Energy Losses and Ranges of Electrons and Positrons." Studies in Penetration of Charged Particles in Matter, pp. 205-268. National Academy of Sciences, National Research Council Publication 1133.

Binks, C., 1969. "Energy Dependence of Lithium Fluoride Dosimeters at Electron Energies from 10 to 35 Mev." Physics in Medicine and Biology, vol. 14, pp. 327-328.

Broszkiewicz, R.K., 1967. "Chemical Dosimetry of Ionizing Radiation." Solid State and Chemical Radiation Dosimetry in Medicine and Biology, pp. 213-240. Symp. Proc., Vienna, 1966. STI/PUB/138. IAEA.

Burch, P.R.J., 1959. "A Theoretical Interpretation of the Effect of Radiation Quality on Yield in the Ferrous and Ceric Sulfate Dosimeters." Radiation Research, vol. 11, pp. 481-497.

Burlin, T.E., 1966. "A General Theory of Cavity Ionisation." British Journal of Radiology, vol. 39, pp. 727-734.

Burlin, T.E., 1968. "Cavity-Chamber Theory." Radiation Dosimetry, chap. 8, vol. I, 2nd ed. Edited by F.H. Attix and W.C. Roesch. Academic Press, New York.

Burlin, T.E., and Chan, F.K., 1967. "Some Applications of Cavity Theory to Condensed-State Radiation Dosimetry." Solid State and Chemical Radiation Dosimetry in Medicine and Biology, pp. 393-405. Symp. Proc., Vienna, 1966. STI/PUB/138. IAEA.

Burlin, T.E., and Chan, F.K., 1970. "The Energy-Size Dependence of the Response of Thermoluminescent Dosimeters to Photon Irradiation." Health Physics, vol. 18, pp. 325-332.

Cameron, J.R., DeWerd, L., Wagner, J., Wilson, C., Doppke, K., and Zimmerman, D., 1967a. "Non-Linearity of Thermoluminescence as a Function of Dose for LiF (TLD-100)." Solid State and Chemical Radiation Dosimetry in Medicine and Biology, pp. 77-89. Symp. Proc., Vienna, 1966. STI/PUB/138. IAEA.

Cameron, J.R., Suntharalingam, N., and Kenny, G.N., 1968. Thermoluminescent Dosimetry. The University of Wisconsin Press, Madison.

Cameron, J.R., and Zimmerman, D.W., 1965. "TL vs R in LiF: A Proposed Mathematical Model." COO-1105-102. USAEC.

Cameron, J.R., and Zimmerman, D.W., 1966. "Modifications of the Mathematical Model Reported in COO-1105-102." COO-1105-113, pt. 1. USAEC.

Cameron, J.R., Zimmerman, D.W., and Bland, R.W., 1967. "Thermoluminescence vs. Roentgens in Lithium Fluoride: A Proposed Mathematical Model." Luminescence Dosimetry, pp. 47-56. Proc. Int. Conf., Stanford, 1965. AEC Symp. Ser., vol. 8. CONF-650637. USAEC.

Cameron, J.R., Zimmerman, D., Kenney, G., Buch, R., Bland, R., and Grant, R., 1964. "Thermoluminescent Radiation Dosimetry Utilizing LiF." Health Physics, vol. 10, pp. 25-29.

Christy, R.W., Johnson, N.M., and Wilbarg, R.R., 1967. "Thermoluminescence and Color Centers in LiF." Journal of Applied Physics, vol. 38, pp. 2099-2106.

Crites, T.R., 1970. "Backscatter of Normally Incident Intermediate Energy Bremsstrahlung from Semi-Infinite Media of Varying Atomic Number." Ph.D. Dissertation, University of Oklahoma, Norman.

Crosby, E.H., Almond, P.R., and Shalek, R.J., 1966. "Energy Dependence of Lithium Fluoride Dosemeters at High Energies." Physics in Medicine and Biology, vol. 11, pp. 131-132.

Eberline Instrument Company, 1969. "TLD Reader Model TLR-5 Technical Manual."

Ehrlich, M., 1970. "Response of Thermoluminescent Dosimeters to 15 Mev Electrons and Cobalt-60 Gamma Rays." Health Physics, vol. 18, pp. 287-289.

Elder, F.R., Gurewitsch, A.M., Langmuir, R.V., and Pollock, H.C., 1947. "A 70 Mev Synchrotron." Journal of Applied Physics, vol. 18, pp. 810-818.

Endres, G.W.R., 1965, "Dosimetry Technology Studies." BNWL-339.

Evans, R.D., 1968. "X-ray and γ-ray Interactions." Radiation Dosimetry, chap. 3, vol. I, 2nd ed. Edited by F.H. Attix and Roesch. Academic Press, New York.

Fowler, J.F., and Attix, F.H., 1966. "Solid State Integrating Dosimeters." Radiation Dosimetry, chap. 13, vol. II, 2nd ed. Edited by F.H. Attix and W.C. Roesch. Academic Press, New York.

Fricke, H., and Hart, E.J., 1966. "Chemical Dosimetry." Radiation Dosimetry, chap. 12, vol. II, 2nd ed. Edited by F.H. Attix and W.C. Roesch. Academic Press, New York.

Fricke, H., and Morse, S., 1927. "The Chemical Action of Roentgen Rays on Dilute Ferrous Sulfate Solutions as a Measure of Dose." American Journal of Roentgenology Radium Therapy Nuclear Medicine, vol. 18, pp. 430-432.

Handbook 55, 1954. "Protection Against Betatron-Synchrotron Radiation up to 100 Million Electron Volts." National Bureau of Standards.

Harshaw Chemical Company, 1971. Private Communication.

Hospital Physicists' Association, 1969. "A Code of Practice for the Dosimetry of 2 to 35 MV X-ray and Caesium-137 and Cobalt-60 Gamma-ray Beams." Physics in Medicine and Biology, vol. 14, pp. 1-8.

Hubbell, J.H., 1969. "Photon Cross Sections, Attenuation Coefficients, and Energy Absorption Coefficients From 10 keV to GeV." National Standard Reference Data System, National Bureau of Standards, 29.

ICRU, 1962. "Clinical Dosimetry." Recommendations of the International Commission on Radiological Units and Measurements, Report 10d. (NBS Handbook 84).

ICRU, 1969. "Radiation Dosimetry: X-rays and Gamma Rays with Maximum Photon Energies Between 0.6 and 50 Mev." Recommendations of the International Commission on Radiological Units and Measurements, Report 14.

Isotopes/Con-Rad, 1968. "Thermoluminescence Dosimetry System Operations Manual."

Isotopes/Con-Rad, 1968a. "Thermoluminescence Dosimetry System Dosimeter Manual."

Johns, H.E., 1961. The Physics of Radiology, 2nd ed. Charles C. Thomas, Springfield.

Jones, D.E., Petrock, K., and Denham, D., 1966. "Thermoluminescent Materials for Personnel Monitoring in Gloved Box Operations." TID-4500, UC-41.

Karzmark, C.J., White, J., and Fowler, J.F., 1964. "Lithium Fluoride Thermoluminescent Dosimetry." Physics in Medicine and Biology, vol. 9, pp. 273-286.

Kastner, J., Hukkoo, R., and Oltman, B.G., 1967. "Lithium Fluoride Thermoluminescent Dosimetry for Beta Rays." Luminescence Dosimetry, pp. 482-489. Proc. Int. Conf., Stanford, 1965. AEC Symp. Ser., vol. 8. CONF-650637. USAEC.

Mayhugh, M.R., 1970. "Color Centers and the Thermoluminescence Mechanism in LiF." Journal of Applied Physics, vol. 41, pp. 4776-4782.

Mason, E.W., 1970. "The Effect of Thermal Neutron Irradiation on the Thermoluminescent Response of Con-Rad Type 7 Lithium Fluoride." Physics in Medicine and Biology, vol. 15, pp. 79-90.

Morehead, F.F., and Daniels, F., 1957. "Thermoluminescence and Coloration of Lithium Fluoride Produced by Alpha Particles, Electrons, Gamma Rays, and Neutrons." The Journal of Chemical Physics, vol. 27, pp. 1318-1324.

Nakajima, T., Hiraoka, T., and Habu, T., 1968. "Energy Dependence of LiF and CaF_2 Thermoluminescent Dosimeters for High Energy Electrons." Health Physics, vol. 14, pp. 266-267.

Naylor, G.P., 1965. "Thermoluminescent Phosphors: Variation of Quality Response with Dose." Physics in Medicine and Biology, vol. 10, pp. 564-565.

Parker, C.V., Blake, K.R., and Nelson, J.B., 1968. "The Response of Thermoluminescent Dosimeters to Protons with Energies to 137 Mev." Proceedings of the Second International Conference on Luminescence Dosimetry, pp. 438-455. Gatlinburg, 1968. CONF-680920. USAEC.

Pinkerton, A.P., Holt, J.G., and Laughlin, J.S., 1966. "Energy Dependence of Lithium Fluoride Dosemeters and High Energy Electrons." Physics in Medicine and Biology, vol. 11, pp. 129-130.

Pinkerton, A., Holt, J.G., Laughlin, J.S., and Almond, P.R., 1967. "Direct Intercomparison of Absorbed Dose by Thermoluminescent Dosimetry." Luminescence Dosimetry, pp. 363-371. Proc. Int. Conf., Stanford, 1965. AEC Symp. Ser., vol. 8. CONF-650637. USAEC.

Reddy, A.R., Ayyangar, K., and Brownell, G.L., 1969. "Thermoluminescence Response of LiF to Reactor Neutrons." Radiation Research, vol. 40, pp. 552-562.

Scharf, K., and Lee, R.M., 1962. "Investigations of the Spectrophotometric Method of Measuring the Ferric Ion Yield in the Ferrous Sulfate Dosimeter." Radiation Research, vol. 16, pp. 115-124.

Schiff, L.I., 1951. "Energy-Angle Distribution of Thin Target Bremsstrahlung." Physical Review, vol. 83, pp. 252-253.

Schulman, J.H., 1967. "Survey of Luminescence Dosimetry." Luminescence Dosimetry, pp. 3-33. Proc. Int. Conf., Stanford, 1965. AEC Symp. Ser., vol. 8. CONF-650637. USAEC,

Schwarz, H.A., 1954. "Temperature Coefficient of the Radiation Induced Oxidation of Ferrous Sulfate." Journal of the American Chemical Society, vol. 76, pp. 1587-1588.

Shalek, R.J., and Smith, C.E., 1969. "Chemical Dosimetry for the Measurement of High-Energy Photons and Electrons." Annals of the New York Academy of Sciences, vol. 161, art. 1, pp. 44-62.

Spinks, J.W.T., and Woods, R.J., 1964. An Introduction to Radiation Chemistry. John Wiley and Sons, Inc., New York.

Suntharalingam, N., 1968. "Thermoluminescence Response of Lithium Fluoride to Radiations of Different LET." Ph.D. Dissertation. University of Wisconsin, Madison.

Suntharalingam, N., and Cameron, J.R., 1968. "Thermoluminescent Response of Lithium Fluoride to Radiations with Different LET." Physics in Medicine and Biology, vol. 14, pp. 397-410.

Suntharalingam, N., and Cameron, J.R., 1969. "Thermoluminescent Response of Lithium Fluoride to High Energy Electrons." Annals of the New York Academy of Sciences, vol. 161, art. 1, pp. 77-85.

Svarcer, V., and Fowler, J.F., 1967. "Spurious Thermoluminescence and Thermoluminescence in Lithium Fluoride Dosimetry Powder." Luminescence Dosimetry, pp. 227-235. Proc. Int. Conf., Stanford, 1965. AEC Symp. Ser., vol. 8. CONF-650637. USAEC.

Tochilin, E., and Goldstein, N., 1966. "Dose Rate and Spectral Measurements from Pulsed X-ray Generators." Health Physics, vol. 12, pp. 1705-1713.

Wagner, J., and Cameron, J.R., 1966. "The Effect of the Quality of Radiation on the Thermoluminescence of LiF (TLD-100)." COO-1105-117. USAEC.

Wingate, C.L., Tochilin, E., and Goldstein, N., 1967. "Response of Lithium Fluoride to Neutrons and Charged Particles." Luminescence Dosimetry, pp. 421-434. Proc. Int. Conf., Stanford, 1965. AEC Symp. Ser., vol. 8. CONF-650637. USAEC.

Worton, R.G., and Holloway, A.F., 1966. "Lithium Fluoride Thermoluminescence Dosimetry." Radiology, vol. 87, pp. 938-943.

Wyckoff, H.O., 1967. "Standards and Quantities in Radiation Dosimetry." Solid State and Chemical Radiation Dosimetry in Medicine and Biology, pp. 333-347. Symp. Proc., Vienna, 1966. STI/PUB/138. IAEA.

Zimmerman, D.W., Rhyner, C.R., and Cameron, J.R., 1966. "Thermal Annealing Effects on the Thermoluminescence of Lithium Fluoride." Health Physics, vol. 12, pp. 525-531.